

AWARD NUMBER: W81XWH-14-1-0281

TITLE: Low-Intensity Vibration as a Treatment for Traumatic Muscle Injury

PRINCIPAL INVESTIGATOR: Dr. Timothy Koh

CONTRACTING ORGANIZATION: University of Illinois at Chicago  
Chicago, IL 60612

REPORT DATE: October 2018

TYPE OF REPORT: Final

PREPARED FOR: U.S. Army Medical Research and Materiel Command  
Fort Detrick, Maryland 21702-5012

DISTRIBUTION STATEMENT: Approved for Public Release;  
Distribution Unlimited

The views, opinions and/or findings contained in this report are those of the author(s) and should not be construed as an official Department of the Army position, policy or decision unless so designated by other documentation.

REPORT DOCUMENTATION PAGE				Form Approved OMB No. 0704-0188	
Public reporting burden for this collection of information is estimated to average 1 hour per response, including the time for reviewing instructions, searching existing data sources, gathering and maintaining the data needed, and completing and reviewing this collection of information. Send comments regarding this burden estimate or any other aspect of this collection of information, including suggestions for reducing this burden to Department of Defense, Washington Headquarters Services, Directorate for Information Operations and Reports (0704-0188), 1215 Jefferson Davis Highway, Suite 1204, Arlington, VA 22202-4302. Respondents should be aware that notwithstanding any other provision of law, no person shall be subject to any penalty for failing to comply with a collection of information if it does not display a currently valid OMB control number. <b>PLEASE DO NOT RETURN YOUR FORM TO THE ABOVE ADDRESS.</b>					
1. REPORT DATE October 2018		2. REPORT TYPE Final		3. DATES COVERED 1 Aug 2014 - 31 Jul 2018	
4. TITLE AND SUBTITLE Low-Intensity Vibration as a Treatment for Traumatic Muscle Injury				5a. CONTRACT NUMBER	
				5b. GRANT NUMBER W81XWH-14-1-0281	
				5c. PROGRAM ELEMENT NUMBER	
6. AUTHOR(S) Timothy Koh; Stefan Judex; Thomas Corbiere  E-Mail: tikoh@uic.edu				5d. PROJECT NUMBER	
				5e. TASK NUMBER	
				5f. WORK UNIT NUMBER	
7. PERFORMING ORGANIZATION NAME(S) AND ADDRESS(ES)  UNIVERSITY OF ILLINOIS at Chicago 809 S MARSHFIELD RM 520 CHICAGO IL 60612-4305				8. PERFORMING ORGANIZATION REPORT NUMBER	
9. SPONSORING / MONITORING AGENCY NAME(S) AND ADDRESS(ES)  U.S. Army Medical Research and Materiel Command Fort Detrick, Maryland 21702-5012				10. SPONSOR/MONITOR'S ACRONYM(S)	
				11. SPONSOR/MONITOR'S REPORT NUMBER(S)	
12. DISTRIBUTION / AVAILABILITY STATEMENT  Approved for Public Release; Distribution Unlimited					
13. SUPPLEMENTARY NOTES					
14. ABSTRACT (~200 words of most sig finding during this period) Traumatic musculoskeletal injuries are among the most common injuries experienced during military combat. Poor healing of traumatic muscle injuries is associated with impaired muscle function, joint stiffness and loss of mobility. Our long-term goal is to develop a device and treatment protocol that provide a safe, inexpensive, and easy to apply treatment that will help to restore normal muscle and joint function to injured military personnel. In this report, we provide preliminary data indicating a trend towards improved healing with LIV. We observed a trend towards a larger fiber area and increased angiogenesis in muscles from LIV-treated mice vs. controls. We have initiated additional experiments to follow up on these findings. Furthermore, initial in vitro studies in macrophages (Mp) demonstrated that these cells are responsive to the LIV signals and that LIV downregulates the expression of pro-inflammatory markers and upregulates the expression of pro-healing markers in Mp. Findings from continued work on this project will provide insight into the potential for LIV as a non-invasive and simple treatment for improving muscle healing, thereby reducing joint stiffness and increasing mobility of polytrauma patients.					
15. SUBJECT TERMS Skeletal muscle repair, low-intensity vibration, monocytes/macrophages, endothelial precursor cells, angiogenesis, myogenesis					
16. SECURITY CLASSIFICATION OF:			17. LIMITATION OF ABSTRACT	18. NUMBER OF PAGES	19a. NAME OF RESPONSIBLE PERSON
a. REPORT	b. ABSTRACT	c. THIS PAGE			USAMRMC
U	U	U	UU	31	19b. TELEPHONE NUMBER (include area code)

## Table of Contents

	<u>Page</u>
<b>1. Introduction.....</b>	<b>4</b>
<b>2. Keywords.....</b>	<b>4</b>
<b>3. Accomplishments.....</b>	<b>4</b>
<b>4. Impact.....</b>	<b>27</b>
<b>5. Changes/Problems.....</b>	<b>28</b>
<b>6. Products.....</b>	<b>28</b>
<b>7. Participants &amp; Other Collaborating Organizations.....</b>	<b>29</b>
<b>8. Appendices.....</b>	<b>32</b>

## **1. INTRODUCTION**

Traumatic skeletal muscle injuries typically result in impaired muscle function, joint stiffness and loss of mobility, which, in turn, results in significant costs for rehabilitation, loss of time for work and reduced combat readiness. Unfortunately, effective treatments for improving the recovery of muscle function and joint mobility are lacking. The proposed Idea Development study is an early-stage investigation into a novel treatment of traumatic muscle injuries – mechanical stimulation via low-intensity vibration (LIV). Mechanical stimulation has an anabolic effect on musculoskeletal tissues, and mechanical stimulation via LIV has been shown to accelerate bone regeneration. Our preliminary data indicate that LIV reduces fibrosis and enhances muscle fiber growth following traumatic muscle injury in mice. Our data also indicate that LIV increases numbers of monocytes and macrophages (Mo/Mp) and endothelial precursor cells (EPC) in the blood; these cells are known to promote healing of muscle injuries. Thus, the central hypothesis of this study is that LIV improves healing of traumatic muscle injuries by increasing the activity of Mo/Mp and EPC in damaged muscle. We will address this hypothesis in three Specific Aims: First, we will determine the effectiveness of locally applied versus whole-body LIV for improving angiogenesis and muscle regeneration and reducing fibrosis. Second, we will determine the role of bone marrow-derived cells (BMDC) in LIV-induced improvements in muscle healing. Third, we will identify specific cells that detect and transduce the LIV signal. If successful, LIV would provide an innovative, non-invasive and simple treatment for improving muscle healing and thereby reducing joint stiffness and increasing mobility of polytrauma patients.

## **2. KEYWORDS**

Skeletal muscle repair, low-intensity vibration, monocytes/macrophages, endothelial precursor cells, angiogenesis, myogenesis

## **3. ACCOMPLISHMENTS**

### **What were the major goals of the project?**

The major goals of this project were divided into three Specific Aims:

1. Determine the effectiveness of locally applied versus whole-body low-intensity vibration (LIV) for improving muscle regeneration following traumatic injury.
2. Determine the role of bone marrow-derived cells (BMDC) in LIV-induced improvements in muscle healing.
3. Identify specific cells that detect and transduce the LIV signal.

### **What was accomplished under these goals?**

#### Specific Aim 1

In the Statement of Work for this project, the goal of Specific Aim 1 is to determine the effectiveness of locally applied versus whole-body low-intensity vibration (LIV) for improving muscle regeneration following traumatic injury. During the first year, approval for animal experiments from the Department of Defense IACUC and the IACUC for the University of Illinois at Chicago (UIC) and Stony Brook University (SBU) was obtained, and the subcontract with SBU was negotiated and signed. In addition, Dr. Eileen Weinheimer-Haus was hired to perform the

experiments associated with Specific Aims 1 and 2. Dr. Weinheimer-Haus performed preliminary experiments to optimize the whole-body LIV signal. For these experiments, mouse gastrocnemius muscles were subjected to laceration injury and then mice were either subjected to daily bouts of whole-body LIV at one of two signals (0.4 g at 45 Hz or 0.2 g at 90 Hz) or handled identically without LIV treatment for controls. Fourteen days after injury, muscles were harvested and healing was assessed. In our preliminary results, no statistically significant differences in healing outcomes were found between LIV-treated mice and non-LIV control mice for both LIV protocols (Figure 1). While we did not see a statistically significant difference between treatment groups, there were trends towards a larger fiber area with both LIV protocols and increased angiogenesis in mice receiving the 0.2 g at 90 Hz LIV compared to controls. Interestingly, we have previously reported an increase in angiogenesis and improved healing with LIV in skin wounds of diabetic mice, who experience impaired angiogenesis and wound healing [1]. Thus, we initiated additional replicate experiments to follow up on these preliminary trends.

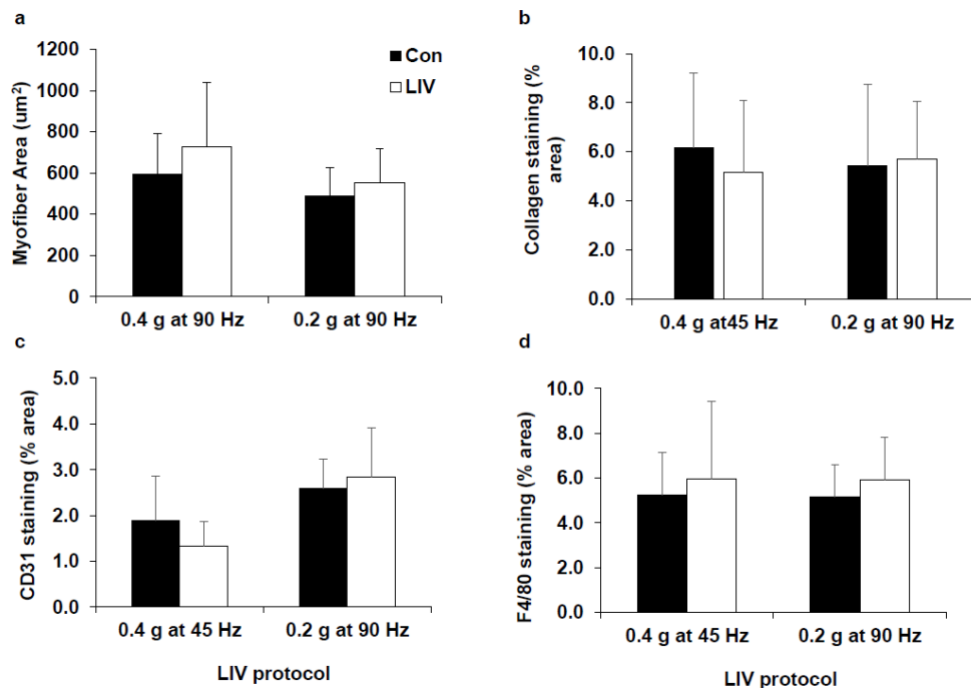


**Figure 1. Effect of two different low-intensity vibration (LIV) signals on muscle healing following laceration injury.** Mouse gastrocnemius muscles subjected to laceration injury and then mice either subjected to 30 minute bouts of whole-body LIV at one of two signals (0.4 g at 45 Hz or 0.2 g at 90 Hz) 5 d/wk or handled identically without LIV treatment for controls. Fourteen days after injury, muscles were harvested and healing was assessed in cryosections stained with (a) hematoxylin and eosin, (b) Masson's Trichrome, (c) CD31 (angiogenesis) and (d) F4/80 (macrophages). Data represent mean  $\pm$  SD, n=7-19 per group.

With the departure of Dr. Eileen Weinheimer-Haus, Mr. Thomas Corbiere was recruited and hired to fill her position. After Mr. Corbiere was trained on the muscle injury technique, he initiated analysis of the tissue samples from the replicate experiment that was performed to follow up on the preliminary trends seen in the first cohort of mice aiming to optimize the whole-body LIV signal. For these experiments, mouse gastrocnemius muscles were subjected to laceration injury and then mice were subjected to daily bouts of whole-body LIV at 0.2 g and 90 Hz or handled identically without LIV treatment for controls. Cohort 2 showed a significant increase in muscle fiber area (Figure 2a). Fiber diameter also showed a trend towards increasing with LIV, although not significantly (Figure 2b). The percentage of normal area showed a significant increase with

vibration (Figure 2d). This data set also showed close to significant decreases ( $p$ -value = 0.078) in the percentage of damaged area at 14 days post injury (Figure 2e). No significant difference was found between LIV and control mice for collagen deposition or angiogenesis (Figure 3a-b). With this most recent data reaffirming the trends we saw from cohort 1, we are reasonably confident that LIV at 0.2 g and 90 Hz leads to improved muscle regeneration following laceration injury as seen by the increased normal area and increased fiber area, although more needs to be tested in regard to the mechanisms and cell types involved as well as other vibration parameters that may be optimal.

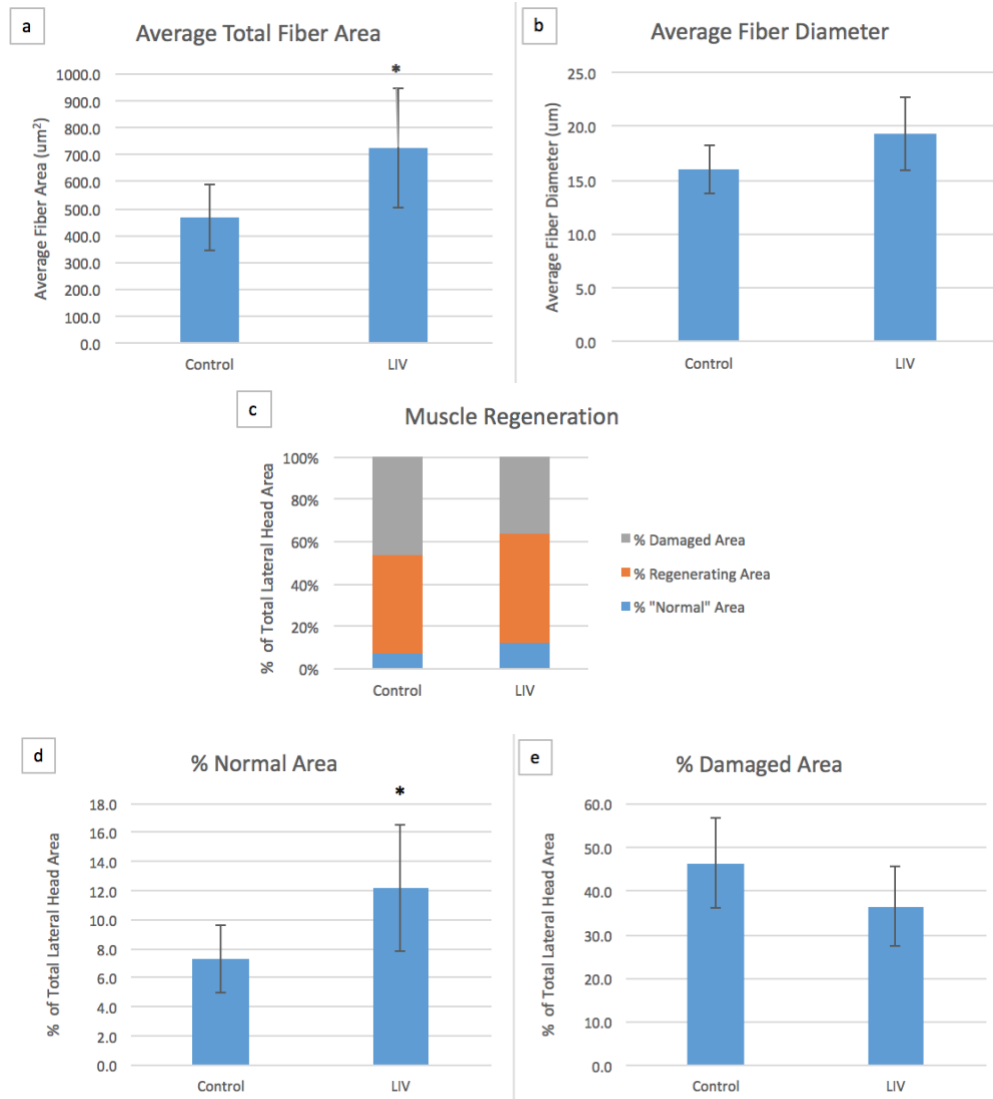


**Figure 2. Effect of low-intensity vibration (LIV) at 0.2 g and 90 Hz on muscle healing following laceration injury.** Mouse gastrocnemius muscles subjected to laceration injury and then mice either subjected to 30 minute bouts of whole-body LIV at 0.2 g at 90 Hz, 5 d/wk or handled identically without LIV treatment for controls. Fourteen days after injury, muscles were harvested and healing was assessed in cryosections stained with hematoxylin and eosin. \*  $p$ -value < 0.05 vs control. Data represent mean  $\pm$  SD,  $n=7-8$  per group.

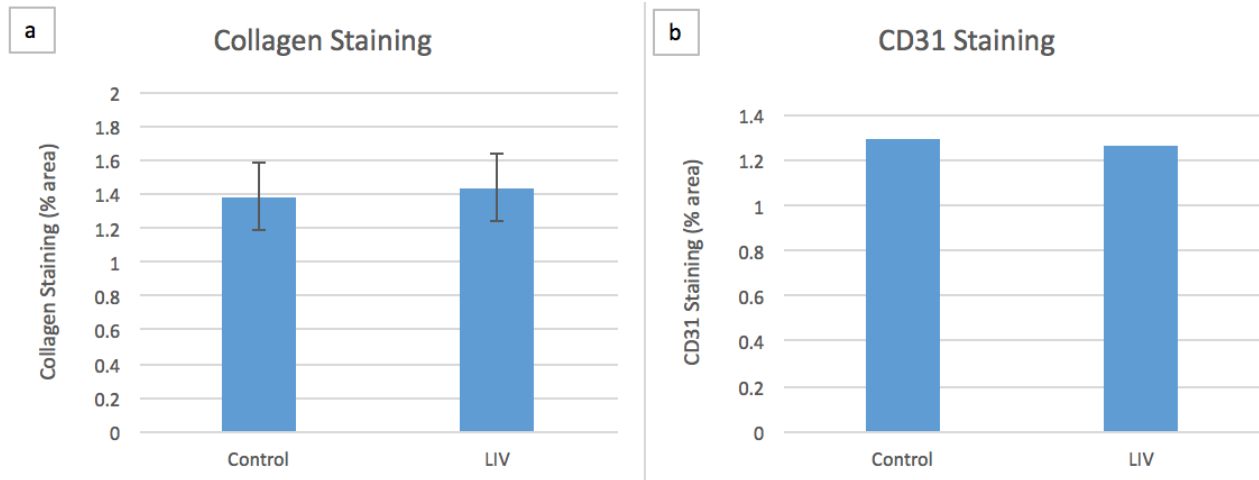


**Figure 3. Effect of low-intensity vibration (LIV) at 0.2 g and 90 Hz on muscle healing following laceration injury.** Mouse gastrocnemius muscles subjected to laceration injury and then mice either subjected to 30 minute bouts of whole-body LIV at 0.2 g at 90 Hz, 5 d/wk or handled identically without LIV treatment for controls. Fourteen days after injury, muscles were harvested and healing was assessed in cryosections stained with (a) Masson's Trichrome, or (b) CD31 (angiogenesis). Data represent mean  $\pm$  SD, n=7-8 per group.

To further investigate Specific Aim 1, Major task 1, subtasks 3 and 4, we performed a similar experiment exploring the effects of LIV on muscle healing using our laceration model of injury. For this experiment, we analyzed muscles harvested at day 7 post-injury. Six mice were given laceration injuries. Three mice were treated with whole body (WBV) LIV (frequency = 90Hz, acceleration = 0.2g) for 7 days and 3 mice were treated identically without LIV. There were no significant differences for tissue morphology, fiber area, fiber diameter, blood vessel formation (CD31), or macrophage accumulation (F4/80) at this time point (Figures 4-8). Taken together with the day 14 data, these results suggest LIV may affect the remodeling phase of tissue repair.

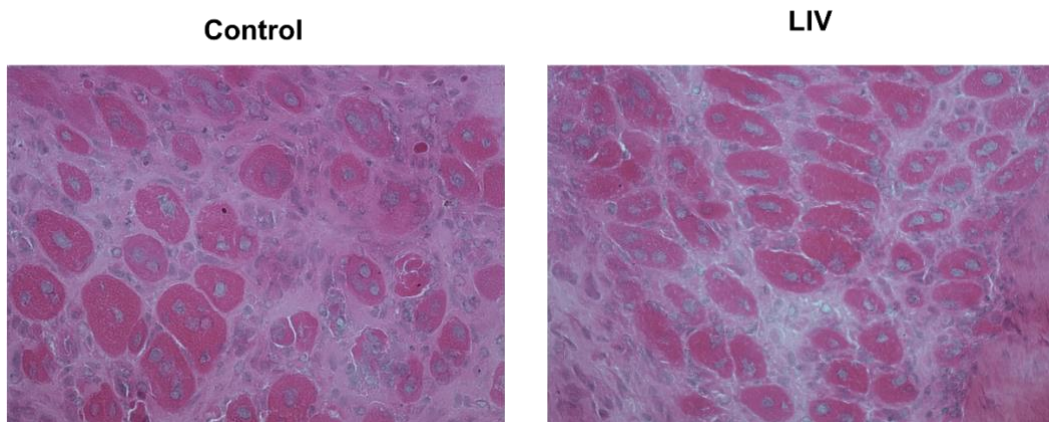


**Figure 4: Effect of low-intensity vibration (LIV) at 0.2 g and 90 Hz on muscle healing on day 7 following laceration injury.** Representative Images at Day 7 Post-Injury. Mouse gastrocnemius muscles subjected to laceration injury and then mice either subjected to 30 minute bouts of whole-body LIV at 0.2 g at 90 Hz, 7 d/wk or handled identically without LIV treatment for controls. Seven days after injury, muscles were harvested and healing was assessed in cryosections stained with hematoxylin and eosin. Images taken at 40x.

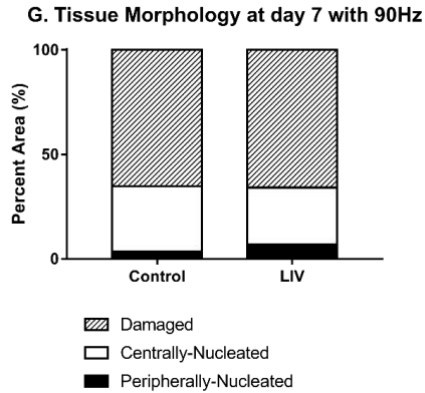


**Figure 5: Effect of low-intensity vibration (LIV) at 0.2 g and 90 Hz on muscle healing on day 7 following laceration injury.** Mouse gastrocnemius muscles subjected to laceration injury and then mice either subjected to 30 minute bouts of whole-body LIV at 0.2 g at 90 Hz, 7 d/wk or handled identically without LIV treatment for controls. Seven days after injury, muscles were harvested and healing was assessed in cryosections stained with hematoxylin and eosin.

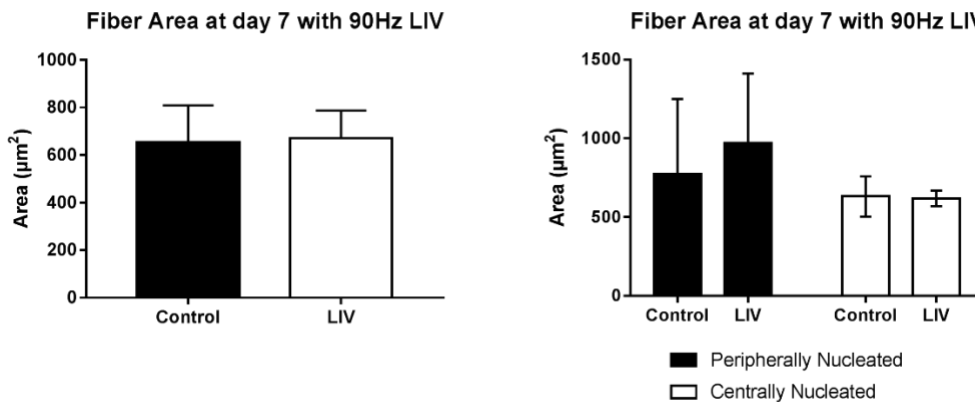


**Figure 6: Effect of low-intensity vibration (LIV) at 0.2 g and 90 Hz on muscle healing on day 7 following laceration injury.** Mouse gastrocnemius muscles subjected to laceration injury and then mice either subjected to 30 minute bouts of whole-body LIV at 0.2 g at 90 Hz, 7 d/wk or handled identically without LIV treatment for controls. Seven days after injury, muscles were harvested and healing was assessed in cryosections stained with hematoxylin and eosin.

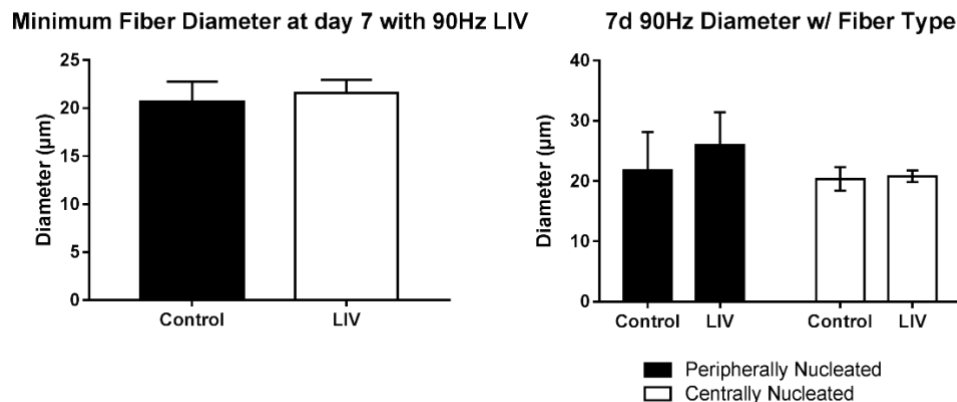


**Figure 7: Effect of low-intensity vibration (LIV) at 0.2 g and 90 Hz on muscle healing on day 7 following laceration injury.** Mouse gastrocnemius muscles subjected to laceration injury and then mice either subjected to 30 minute bouts of whole-body LIV at 0.2 g at 90 Hz, 7 d/wk or handled identically without LIV treatment for controls. Seven days after injury, muscles were harvested and healing was assessed in cryosections stained with hematoxylin and eosin.



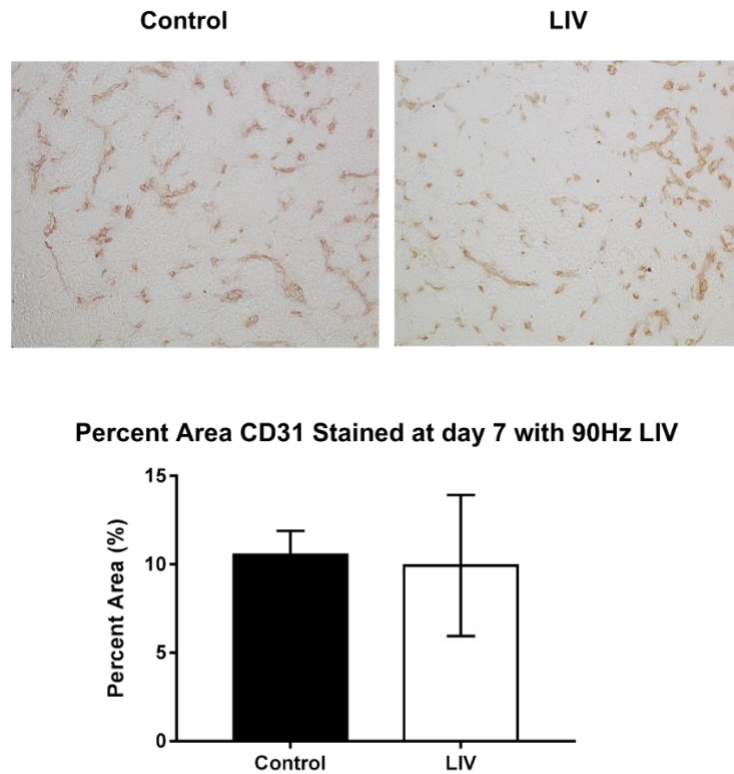


**Figure 8: Effect of low-intensity vibration (LIV) at 0.2 g and 90 Hz on angiogenesis on day 7 following laceration injury.** Mouse gastrocnemius muscles subjected to laceration injury and then mice either subjected to 30 minute bouts of whole-body LIV at 0.2 g at 90 Hz, 7 d/wk or handled identically without LIV treatment for controls. Seven days after injury, muscles were harvested and angiogenesis was assessed in cryosections stained with CD31.

After determining the effectiveness of whole-body LIV, we performed an experiment exploring the effects of local LIV on muscle healing using our laceration model of injury. Twelve mice were given laceration injuries. Six mice were treated with local LIV (frequency = 90Hz, acceleration = 0.2g) for 14 days and 6 mice were treated identically without LIV. Due to the number of mice that fit on the machine, we performed 2 trials with 6 mice each. Figures 9 and 10 show images of the local LIV device applying a signal to the legs of the mice. There was a significant decrease in damaged area and a significant increase in peripherally nucleated area with the application of local LIV (Figure 11 and 12). Average fiber area and peripherally nucleated fiber area increased with LIV while centrally nucleated fiber area showed a trend towards increasing ( $p = 0.08$ ) (Figure 13). Average, peripherally nucleated, and centrally nucleated fiber areas all increased significantly with the application of LIV (Figure 14). Based on these robust differences and the consistency of this data set, we have decided to use the local LIV at 90 Hz and 0.2g protocol for all in vivo experiments moving forward.

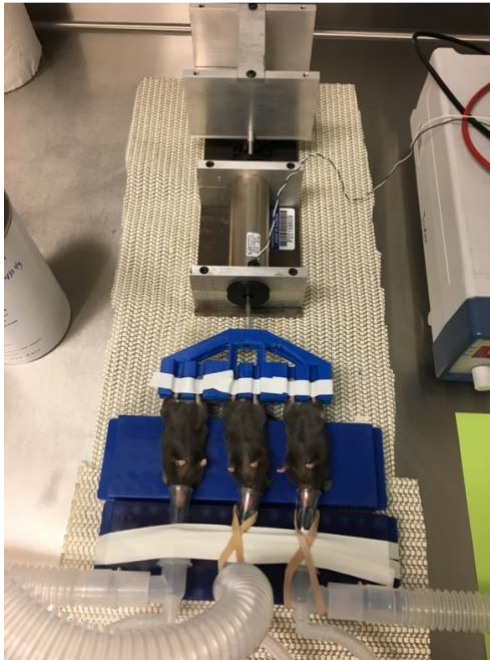


**Figure 9:** Local LIV device with mice being treated



**Figure 10:** Closer view of mice on Local LIV device

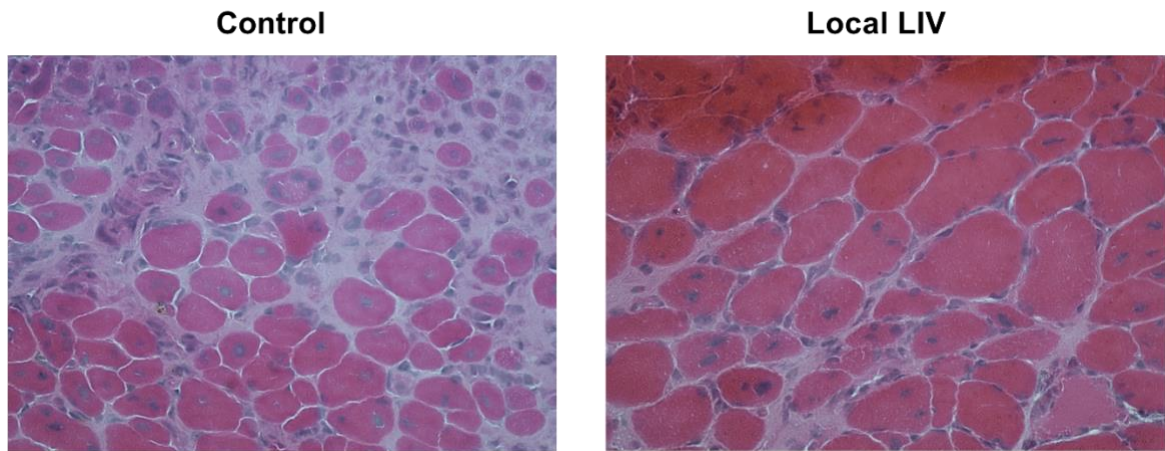


**Figure 11: Effect of locally applied low-intensity vibration (LIV) at 0.2 g and 90 Hz on muscle healing on day 14 following laceration injury.** Mouse gastrocnemius muscles subjected to laceration injury and then mice either subjected to 30 minute bouts of locally applied LIV at 0.2 g at 90 Hz, 7 d/wk or handled identically without LIV treatment for controls. Fourteen days after injury, muscles were harvested and healing was assessed in cryosections stained with hematoxylin and eosin. Representative Images at Day 14 Post-Injury. Images taken at 40x.

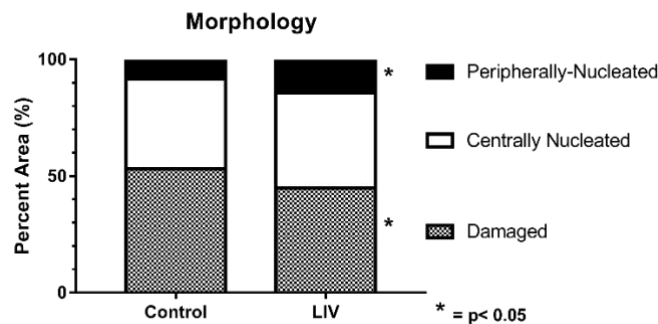


**Figure 12: Effect of locally applied low-intensity vibration (LIV) at 0.2 g and 90 Hz on muscle healing on day 14 following laceration injury.** Mouse gastrocnemius muscles subjected to laceration injury and then mice either subjected to 30 minute bouts of locally applied LIV at 0.2 g at 90 Hz, 7 d/wk or handled identically without LIV treatment for controls. Fourteen days after injury, muscles were harvested and healing was assessed in cryosections stained with hematoxylin and eosin.

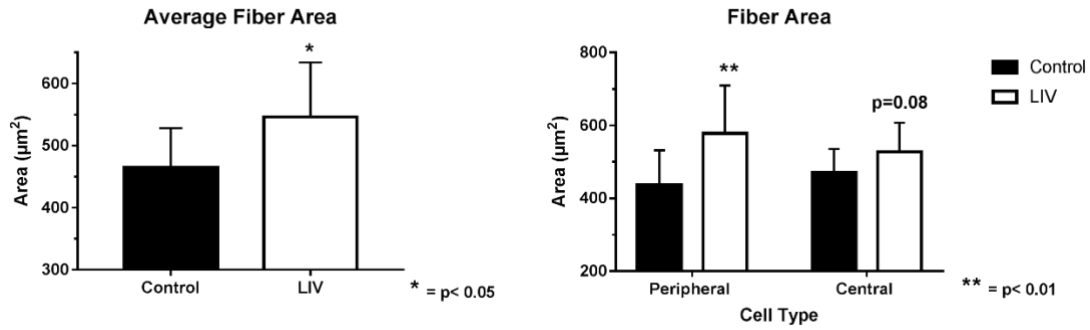


**Figure 13: Effect of locally applied low-intensity vibration (LIV) at 0.2 g and 90 Hz on muscle healing on day 14 following laceration injury.** Mouse gastrocnemius muscles subjected to laceration injury and then mice either subjected to 30 minute bouts of locally applied LIV at 0.2 g at 90 Hz, 7 d/wk or handled identically without LIV treatment for controls. Fourteen days after injury, muscles were harvested and healing was assessed in cryosections stained with hematoxylin and eosin.

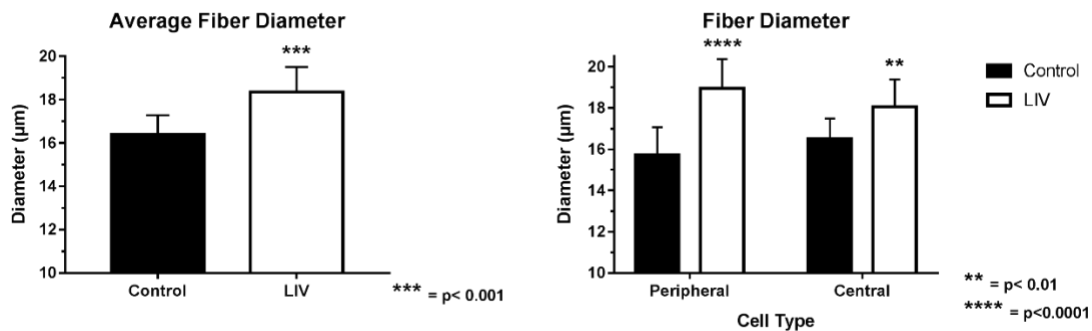


**Figure 14: Effect of locally applied low-intensity vibration (LIV) at 0.2 g and 90 Hz on muscle healing on day 14 following laceration injury.** Mouse gastrocnemius muscles subjected to laceration injury and then mice either subjected to 30 minute bouts of locally applied LIV at 0.2 g at 90 Hz, 7 d/wk or handled identically without LIV treatment for controls. Fourteen days after injury, muscles were harvested and healing was assessed in cryosections stained with hematoxylin and eosin.

Additionally, Dr. Koh has established a collaboration with Dr. Onur Bilgen at Rutgers University to develop an alternative method for applying LIV locally. Dr. Bilgen is a mechanical engineer with an expertise in vibration energy. A prototype has been developed and we have met with a cohort of students and professionals in the MAD Lab at the UIC Innovation Center (<https://madlab.uic.edu/>) for feedback and design ideas. We are currently exploring the most appropriate applications for this device. We plan to use this device in experiments as an alternative mode of locally delivered LIV in the future.

In the Statement of Work, the goal of Specific Aim 1, Major task 2 is to determine the relative effectiveness of early versus late application of LIV for improving muscle healing. For these experiments, mouse gastrocnemius muscles were subjected to laceration injury and mice then received either whole-body LIV (0.4 g at 45 Hz for 30 min/d, 5 d/wk) starting on day 14 post-injury or were handled identically without LIV treatment for controls. Muscles were collected at day 28 post-injury (14 days after initiation of LIV treatment) and healing was assessed. Preliminary results suggest that initiating LIV treatment 14 days post-injury does not appear to alter the healing response compared to control mice (Figure 15). The average minor fiber diameter (a measure of fiber size), muscle fibrosis and angiogenesis were not different between control and LIV groups.

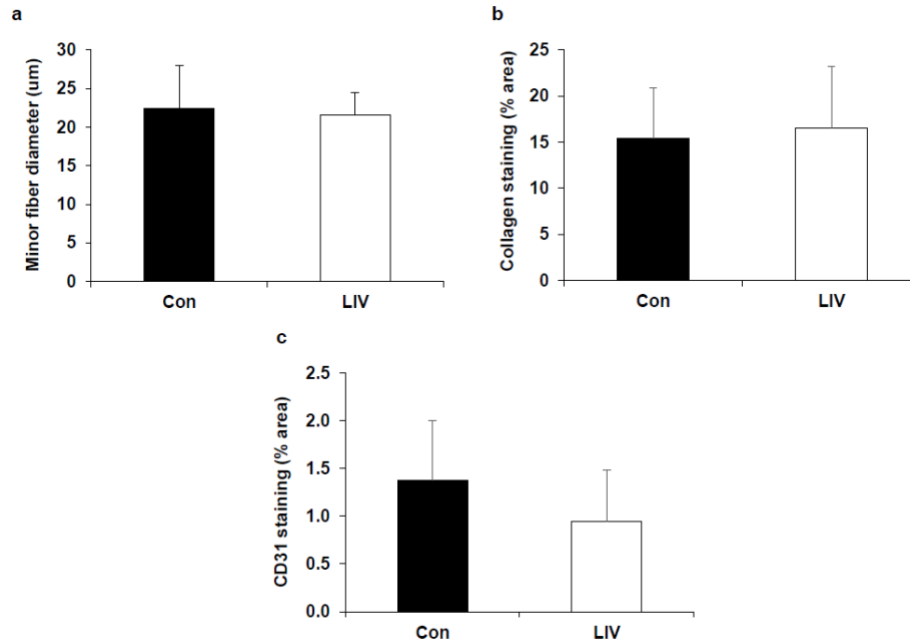


**Figure 15. Effect of late application low-intensity vibration (LIV) signals on muscle healing following laceration injury.** Mouse gastrocnemius muscles subjected to laceration injury and then mice subjected to either whole-body LIV (0.4 g at 45 Hz for 30 min/d, 5 d/wk) starting on day 14 post-injury or handled identically without LIV treatment for controls. On day 28 after injury, muscles were harvested and healing was assessed in cryosections stained with (a) hematoxylin and eosin, (b) Masson's Trichrome and (c) CD31 (angiogenesis). Data represent mean  $\pm$  SD, n=6-8 per group.

As seen in some of the above histological data, the laceration model of injury being used to investigate Specific Aim 1 has some inherent variability which makes obtaining consistent results challenging. In an effort to deal with this, we developed a similar model of injury that can be used with MRI analysis. MRI analysis allows us to analyze inflammation, necrosis, and fibrosis non-invasively in a serial manner over the time course of healing providing more consistent analysis. However, our previous laceration model of injury does not generate a large enough volume injury to be consistently detected by MRI. Thus, rather than using a scalpel to make a thin laceration through the lateral gastrocnemius muscle, we are testing the use of a 3 mm biopsy punch to create an injury with a larger volume that is more easily detectable with MRI. We also expect this model of injury to be even more representative of traumatic muscle injury induced by a projectile than the current model. Representative MRI images have been included using the original model of laceration (Figure 16).

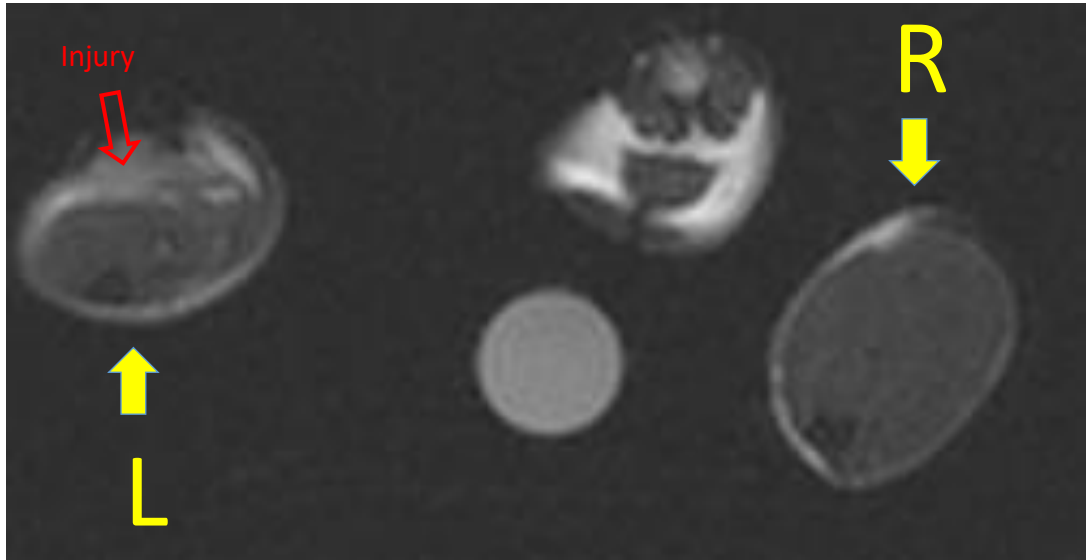


**Figure 16. Magnetic Resonance Imaging of muscle laceration injury with T2 contrast and gadolinium enhancement.** Mouse gastrocnemius muscles were subjected to laceration injury and scanned using MRI 2 days post-injury. In this image, the left (L) gastrocnemius was injured while the right (R) gastrocnemius was left uninjured. Using T2 contrast, areas of bright contrast represent inflammation (indicated by red arrow) and edema within the muscle while darker areas show normal muscle tissue. Area and volume measurements can be taken using these images in a serial manner over various time points.

Using this biopsy punch model, we performed an experiment using the punch model of VML injury along with MRI analysis. Eight mice were injured and either treated with whole-body LIV at 0.2g and 90 Hz or handled identically without LIV treatment. T2 images, which capture edema and inflammation, shows obvious changes within the injured muscle over time from 2 to 22 days post injury. Unfortunately, using this model of traumatic muscle injury, LIV is not showing any significant differences from the control group when looking at area, volume, or T2 signal intensity measurements (Figure 17-21). This could mean that this particular model creates too severe of an injury that cannot be improved with LIV alone and/or the MRI analysis is not sensitive enough to detect those differences. All in all, we are excited about the development of our new model of VML injury and the usefulness of MRI analysis.

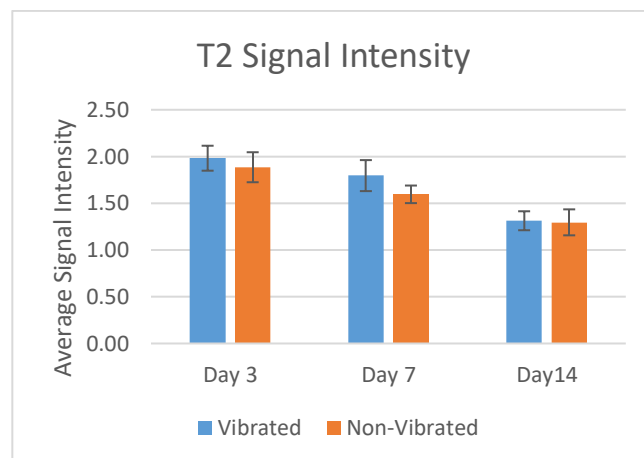


**Figure 17: T2 Signal Intensity over days 3, 7, and 14.** T2 Signal Intensity is a measure of edema and inflammation. Values have been normalized to the signal intensity of the uninjured contralateral leg. Reduction of the signal intensity occurs over the time course.

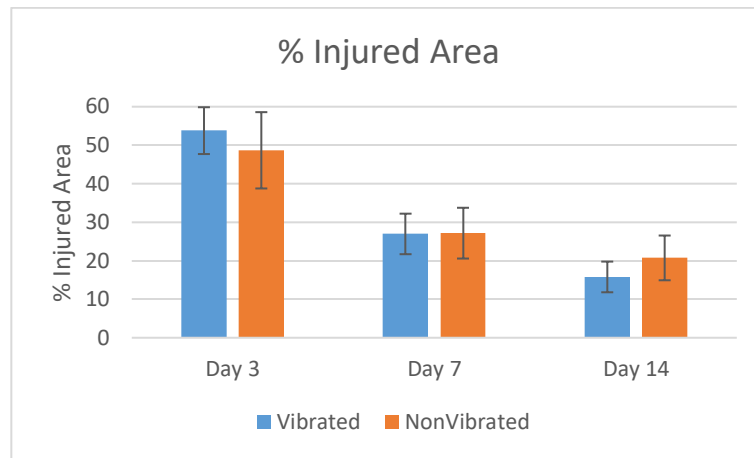


**Figure 18:** Percent Injured Area over days 3, 7, and 14. Values were calculated by dividing the injured area by the entire area of the injured gastrocnemius muscle. The injury as detected by T2 signal intensity decreases from day 3 to day 14. Reduction of the injured area occurs over this time course.

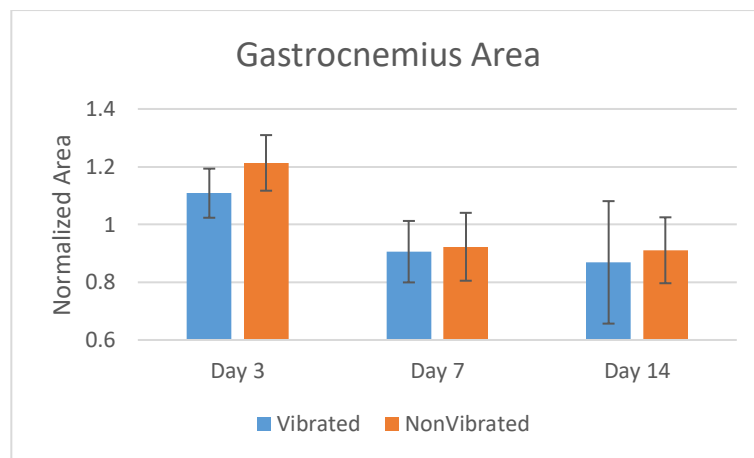


**Figure 19:** Area of the injured gastrocnemius. Values were obtained by measuring the area of the injured gastrocnemius on corresponding representative images. Selected images were determined based on anatomical landmarks. Day 3 shows obvious increased volume due to inflammation that subsides by day 7 and 14.

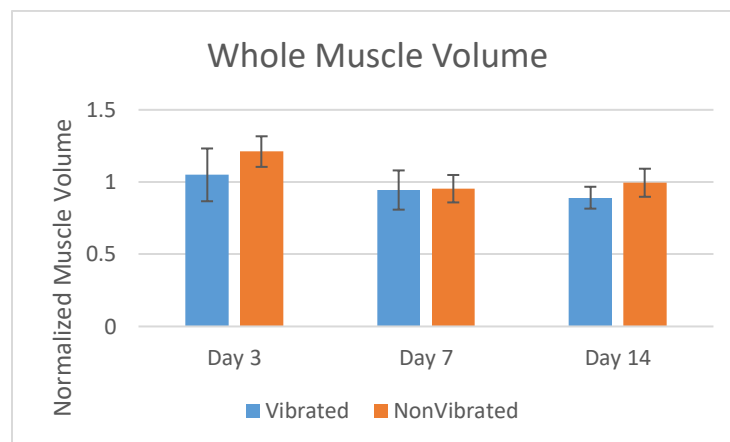


**Figure 20:** Injured Muscle Volume. Values were normalized to the uninjured contralateral leg.

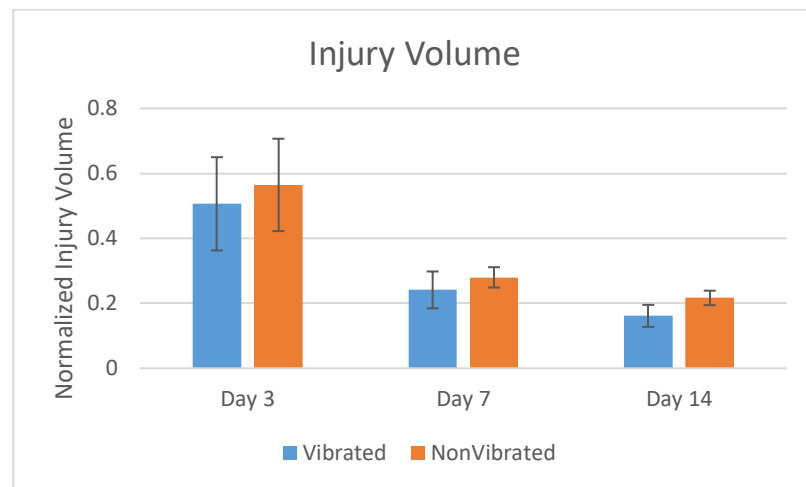


**Figure 21:** Injury Volume. Values were normalized to the uninjured contralateral leg.

Gastrocnemius muscles from the previous experiment were harvested on day 23 post-injury from both LIV-treated and sham-treated mice. Histological analysis was performed. No significant differences were detected for % damaged area, % regenerating area, % normal area, fiber diameter or number of fibers (Figures 22-24). There was a significant difference between the LIV group and control for fiber area (Figure 25), which is an opposite effect from previous experiments using the laceration model. Thus, the positive effect of LIV on muscle fiber area maybe limited to non-volumetric injuries. Muscles were analyzed for collagen deposition using Masson's trichrome. Measurements were taken for % area stained, staining intensity, and staining intensity variation and no significant differences were detected between LIV and control (Figures 26-28). Staining for CD31 and F4/80 were performed. No significant difference was found in CD31 staining between treatment and control. F4/80 staining was not intense enough at day 23 to warrant analysis. This most likely means that staining for F4/80 is more appropriate at earlier time points.

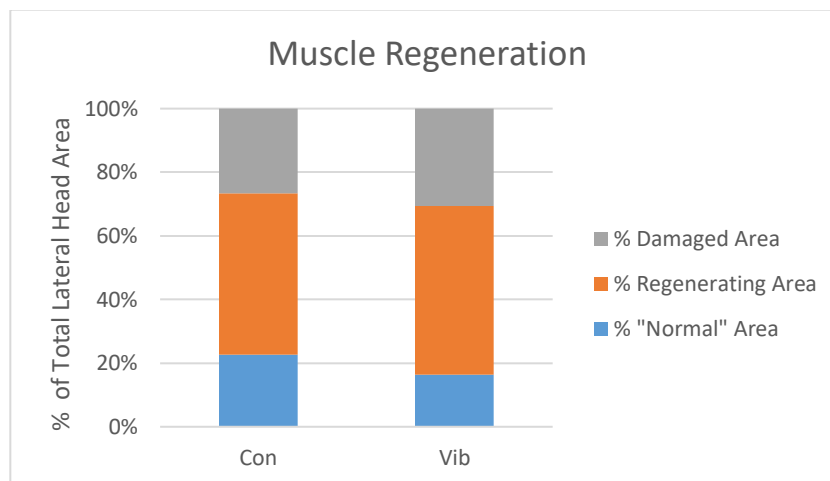


**Figure 22:** Muscle Regeneration at day 23 post-VML injury.



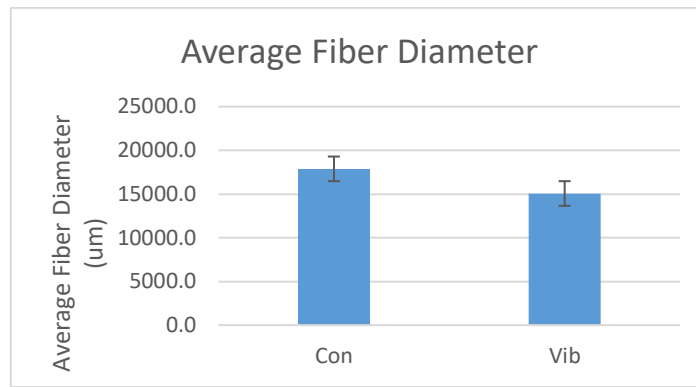


**Figure 23:** Average Myofiber diameter at day 23 post-VML injury.

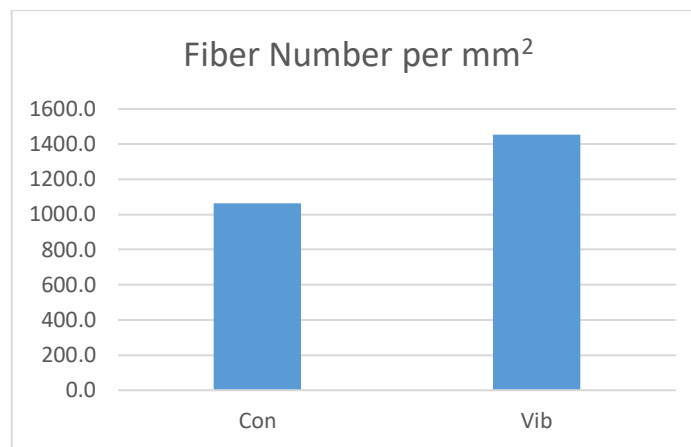


**Figure 24:** Number of myofibers per mm<sup>2</sup> at day 23 post-VML injury

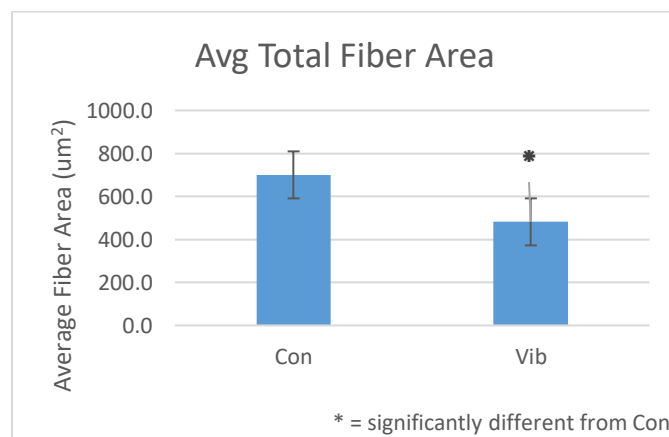


**Figure 25:** Average Myofiber Area at day 23 post-VML injury

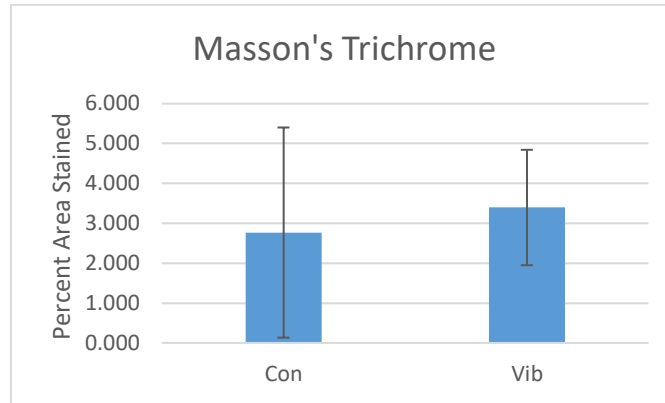


**Figure 26:** Percent Area Stained for Collagen at day 23 post-VML injury

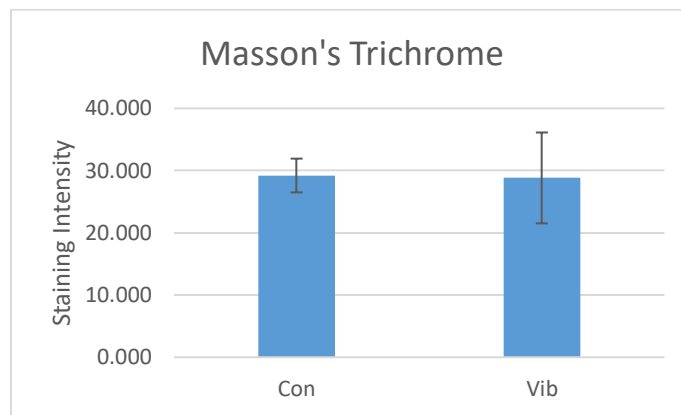


**Figure 27:** Collagen Staining Intensity at day 23 post-VML injury

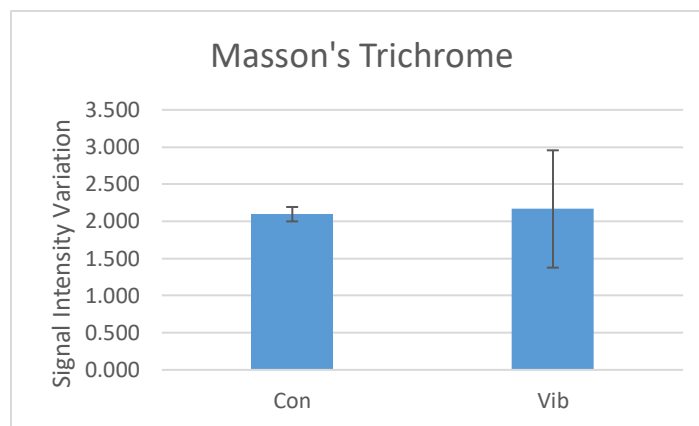


**Figure 28:** Collagen Staining Intensity Variation at day 23 post-VML injury

Optimizing protocols for analysis of tissues harvested from the Local vibration experiment at day 14 using IHC and IF is ongoing. Markers are being determined and tested for satellite cell accumulation (Pax7, SM/C-2.6), early myoblast proliferation (MyoD), early myofiber growth (F1.652/embryonic myosin), mature myofiber growth(MF-20/adult myosin) , and neural integration (alpha-bungaritoxin/Ach receptors, beta-tubulin III/axonal growth) Representative images for embryonic myosin using the F1.652 antibody are shown in Figure 29 and 30 for day 7 and day 14.

Note the presence of embryonic myosin at day 7 and the absence at day 14 with the maturation of the myofibers.

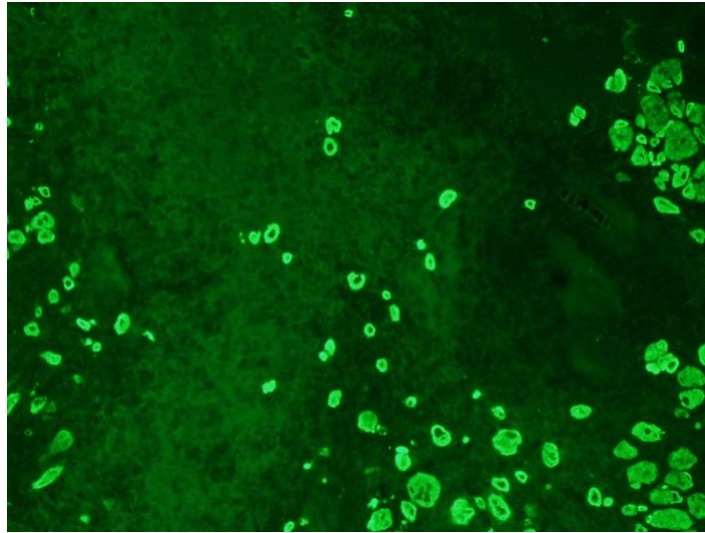


**Figure 29:** Embryonic myosin staining using F1.652 antibody at day 7. This image has many bright green areas that are stained positive for embryonic myosin which indicates myofibers that are in the early stages of regeneration. Image was taken at 10x.

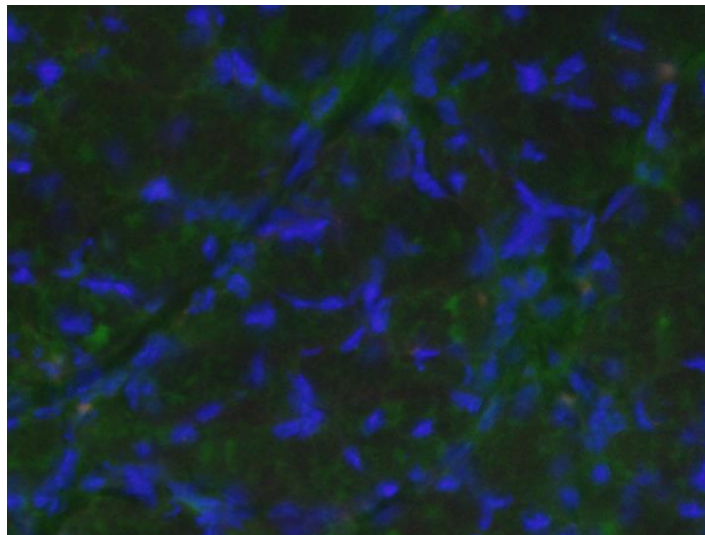


**Figure 30:** Embryonic myosin staining using F1.652 antibody at day 14. This image lacks bright green areas that are stained positive for embryonic myosin which indicates that myofibers at this time point are not in the early stages of regeneration. Blue staining is DAPI. Image was taken at 40x.

### References

1. Weinheimer-Haus EM, Judex S, Ennis WJ, Koh TJ (2014) Low-intensity vibration improves angiogenesis and wound healing in diabetic mice. PLoS One 9: e91355.

## Specific Aim 2

In the Statement of Work for this project, the goal of Specific Aim 2 is to determine the role of bone marrow-derived cells (BMDC) in LIV-induced improvements in muscle healing. In vitro LIV experiments were performed in murine macrophages (J774.1) to evaluate the effect of varying LIV signals on cell viability, proliferation, and phenotype. For these experiments, two different LIV signal frequencies (30 Hz or 100 Hz) were combined with two acceleration magnitudes (0.15 g or 1 g) to generate four distinct LIV signals. Murine macrophages were exposed to each of the four different LIV signals for 20 min per session for 2 sessions/day. Cell viability was unaffected by LIV, but proliferation was increased by each of the four LIV signals on days 1, 2, and 3 (Figure 31). The 100 Hz/0.15g signal appeared to be the most effective signal. In addition, mRNA expression of the pro-angiogenic growth factor VEGF and pro-healing growth factor TGF- $\beta$  were higher in LIV-treated cells vs. non-LIV controls (Figure 32). For VEGF, the greatest increase in expression was with the 100 Hz/0.15g protocol, while there were no significant differences between individual LIV groups for TGF- $\beta$  expression. Flow cytometric analysis of pro-inflammatory and pro-healing markers revealed a lower expression of the inflammatory markers IL-6, TNF- $\alpha$ , IFN- $\gamma$  and GM-CSF (Figures 33) and a higher expression of the pro-healing markers IL-10 and M-CSF (Figure 34) in macrophages treated with LIV vs. control. Collectively, these data demonstrate that macrophages are responsive to high-frequency oscillations applied at low intensities and that LIV downregulates the expression of pro-inflammatory markers and upregulates the expression of pro-healing markers in macrophages in vitro.

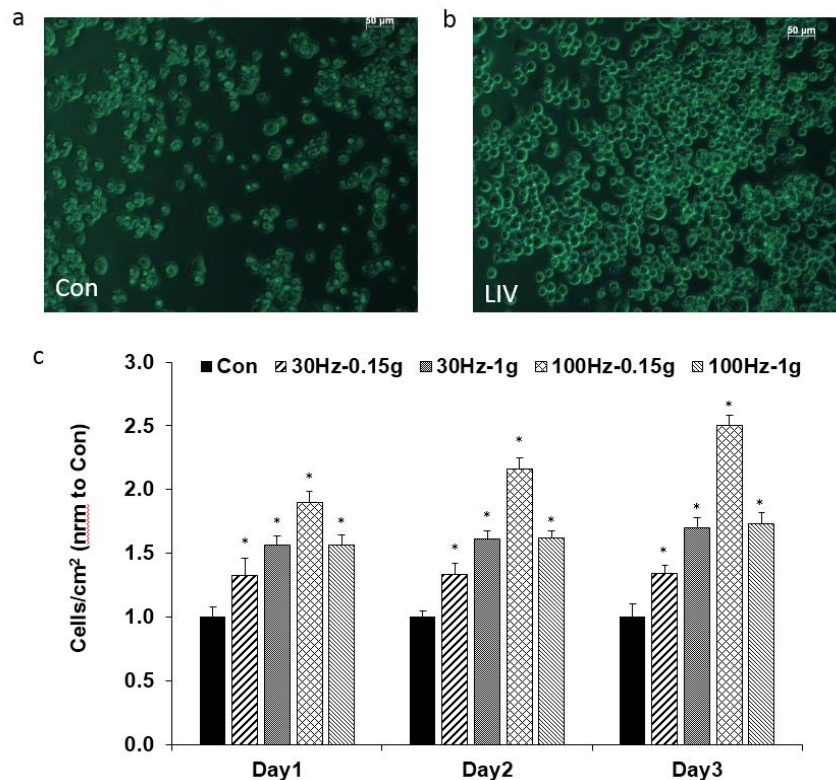


**Figure 31: Effect of LIV on macrophage viability and proliferation in vitro.** (a and b) Fluorescent images of J774.1 murine macrophages double stained with Calcein AM (green) and Ethidium Homodimer (red). Cells received non-LIV sham treatment (a) or LIV at 100Hz-0.15g (b). Viable cells in green demonstrate that LIV is not cytotoxic. (c) Cell density of macrophages under LIV and non-LIV conditions over 3 days. \* $p < 0.05$  vs Con.

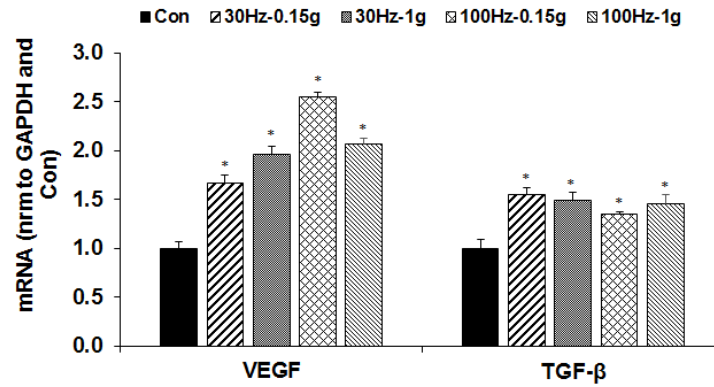


**Figure 32: Effect of LIV on gene expression of growth factors in macrophages in vitro.** Gene expression of pro-angiogenic growth factor VEGF and pro-healing growth factor TGF-β in macrophages treated with non-LIV sham (Con) or LIV. \*p<0.05 vs Con.

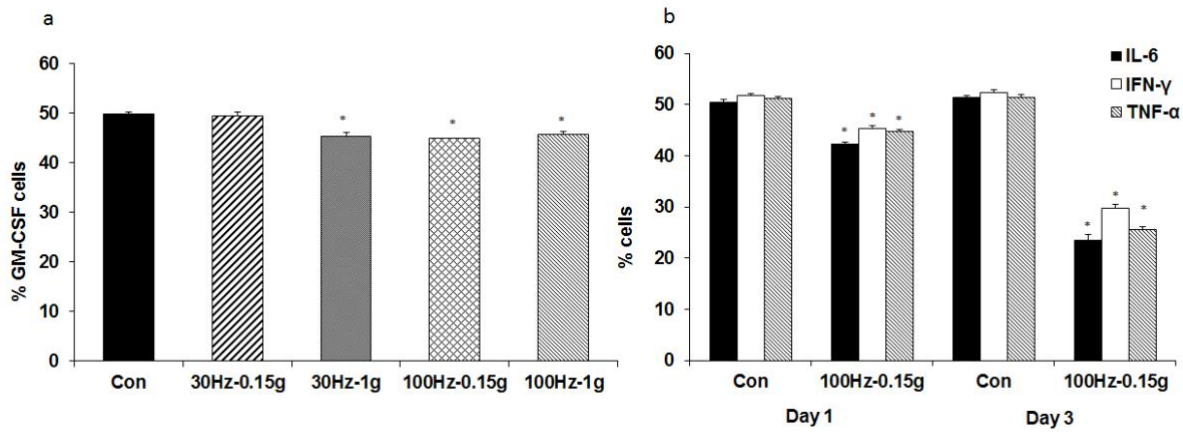


**Figure 33: Effect of LIV on expression of pro-inflammatory markers in macrophages in vitro.** Flow cytometric analysis of macrophages positive for pro-inflammatory markers (a) GM-CSF and (b) IFN-γ, IL-6, and TNF-α in non-LIV and LIV (100Hz-0.15g)-treated cells. \*p<0.05 vs Con.

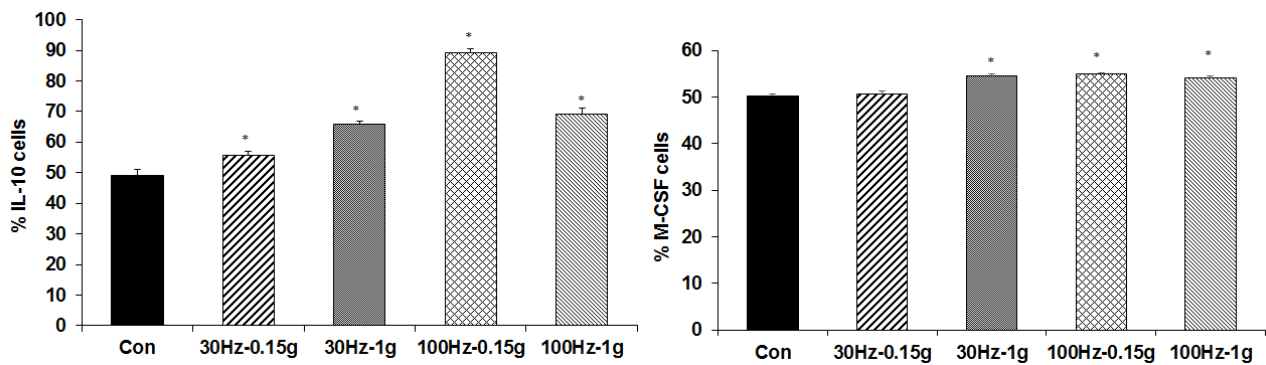


**Figure 34: Effect of LIV on expression of pro-healing markers in macrophages in vitro.** Flow cytometric analysis of macrophages positive for pro-healing markers (a) IL-10 and (b) M-CSF in non-LIV and LIV (100Hz-0.15g)-treated cells. \*p<0.05 vs Con.

In vivo experiments were performed in which mouse gastrocnemius muscles were subjected to laceration injury and then mice were subjected to daily bouts of whole-body LIV at 0.2 g and 90 Hz or handled identically without LIV treatment for controls. Seven and fourteen days after injury, muscles were harvested and healing was assessed. Macrophage accumulation showed no change with LIV at day 7 (Figure 35) and a trend towards increasing with LIV at day 14 (Figure 36), however, high variability prevented this trend from becoming significant. These trends alongside the in vitro data suggest that macrophages may play a role in the response to LIV.

In the experiment using the punch model described in specific aim 1, F4/80 staining was not intense enough at day 23 to warrant analysis. This most likely means that staining for F4/80 is more appropriate at earlier time points.

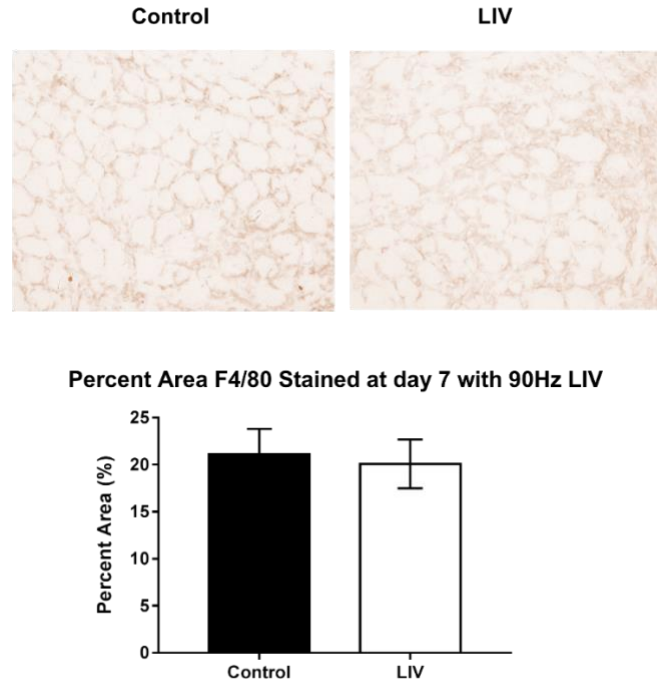


**Figure 35: Effect of low-intensity vibration (LIV) at 0.2 g and 90 Hz on macrophage accumulation on day 7 following laceration injury.** Mouse gastrocnemius muscles subjected to laceration injury and then mice either subjected to 30 minute bouts of whole-body LIV at 0.2 g at 90 Hz, 7 d/wk or handled identically without LIV treatment for controls. Seven days after injury, muscles were harvested and macrophage accumulation was assessed in cryosections stained with F4/80.



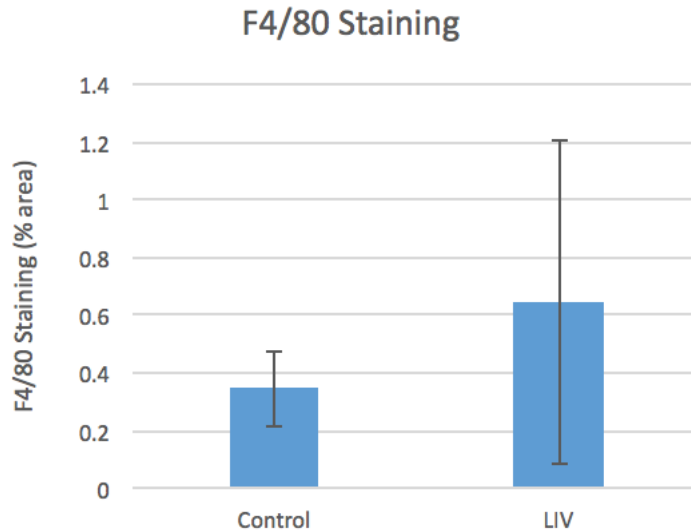


**Figure 36. Effect of low-intensity vibration (LIV) at 0.2 g and 90 Hz on muscle healing following laceration injury.** Mouse gastrocnemius muscles subjected to laceration injury and then mice either subjected to 30 minute bouts of whole-body LIV at 0.2 g at 90 Hz, 5 d/wk or handled identically without LIV treatment for controls. Fourteen days after injury, muscles were harvested and healing was assessed in cryosections stained with F4/80 (macrophages). Data represent mean  $\pm$  SD, n=7-8 per group.

In the statement of work, Specific Aim 2 was proposed with 3 major tasks. The goal of Major Task 1 was to determine whether LIV increases mobilization and homing of monocytes/macrophages (Mo/Mp), endothelial precursor cells (EPC) and hemopoietic stem and precursor cells (HSPC) following traumatic muscle injury. The goal of major task 2 was to determine whether LIV enhances the pro-angiogenic and pro-healing phenotype of Mo/Mp, EPC and HSPC following traumatic muscle injury. The goal of Major Task 3 was to determine whether ablation of Mo/Mp blunts LIV-induced healing. Unfortunately, we ran out of time to complete these experiments within the reporting period of the grant, however we are still planning on performing them in the future.

### Specific Aim 3

In the Statement of Work for this project, the goal of Specific Aim 3 is to identify specific cells that detect and transduce the LIV signal. The results of the in vitro experiment described under Specific Aim 2 with the J774 cells is also relevant here. Data from this experiment demonstrated that macrophages are responsive to high-frequency oscillations applied at low intensities and that LIV downregulates the expression of pro-inflammatory markers and upregulates the expression of pro-healing markers in macrophages in vitro.

Preliminary in vitro experiments were performed with C2C12 cells in order to optimize conditions. These experiments are aimed at determining the effect of LIV on C2C12 cell proliferation and differentiation. We optimized techniques to analyze the effect of LIV on myotube formation, size, and maturation using fluorescent imaging techniques. We also optimized protein quantification assays to identify the mechanisms involved in the LIV induced improvements in healing. Figure 37 shows pictures of the LIV device vibrating a chamber slide for imaging and a 12-well plate for protein assays.

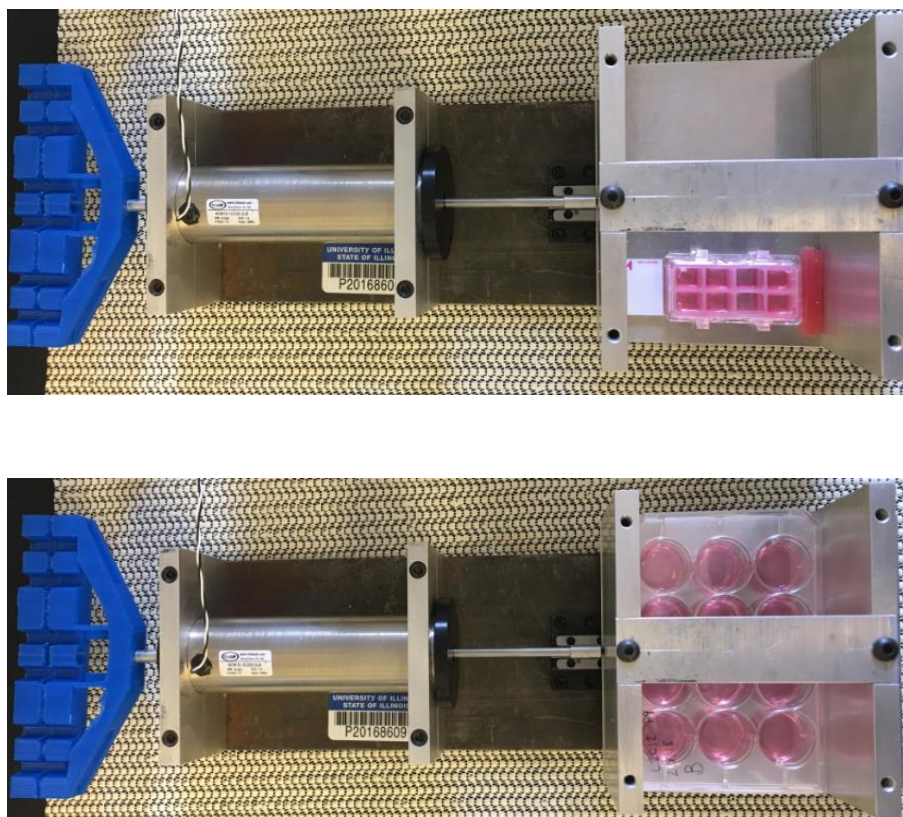


**Figure 37:** The LIV device vibrating a chamber slide (top) for imaging cells and a 12-well plate (bottom) for protein/RNA assays.

Protein assay optimization – We will quantify total protein concentration by using the filter paper assay from Minamide and Bamberg, Anal Biochem, 1990. We have had success with it from previous experiments and is an assay that is compatible with the detergents included in our lysis buffer. Figure 38 shows the filter paper assay in progress. The left three columns are the BSA protein standard and all other squares are samples. The intensity of the blue color can provide qualitative feedback (lighter blue = less protein, darker blue = more protein). The dye from each square is extracted into a microwell plate and quantified by absorbance on a plate reader. Other assays such as Pierce 660 had issues with buffer compatibility as well as the working range of the standard dilutions. We have completed a preliminary experiment to determine the optimal seeding density for our 6-well plates and successfully ran the filter paper assay using these samples.



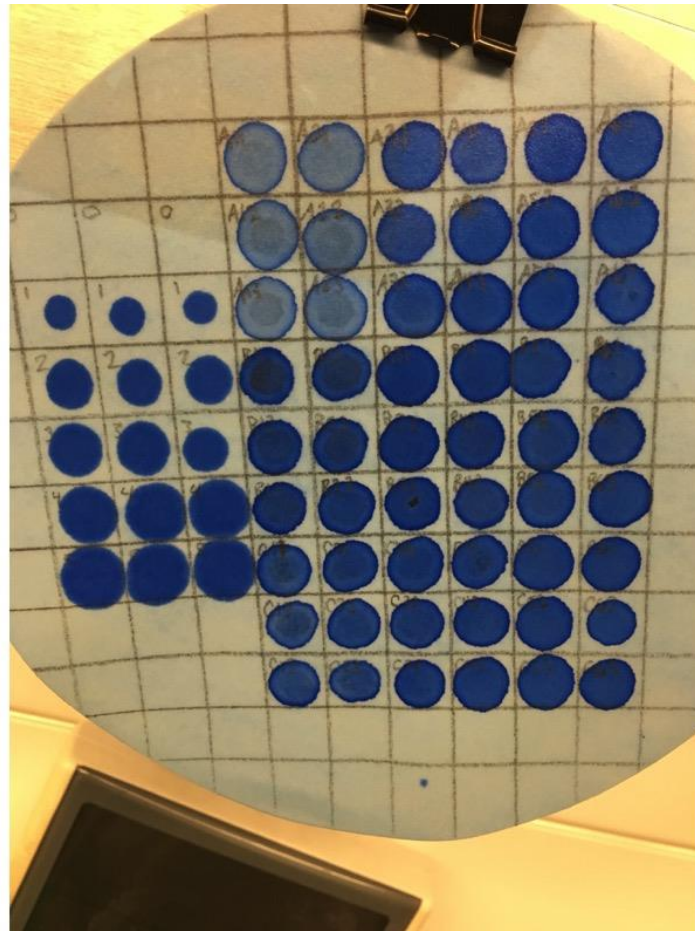


**Figure 38:** Filter Paper Assay for total protein quantification

We have been determining the optimal surface on which to grow C2C12 cells that shows similar cell behavior to standard culture plates. After growing cells on a variety of surfaces and implements such as permanox chamber slides, glass chamber slides, and coated coverslips, we have determined that cells grown on the permanox plastic chamber slides were the most optimal. Preliminary experiments have been performed to determine optimal grown conditions. We have also run a time course of cells grown in differentiation medium over 2, 4, and 6 days. Cells were stained for actin and myosin. Sample images have been included in Figure 39. These images will be analyzed for myotube formation, size, and maturation. We are also optimizing protocols for staining other markers related to regeneration such as Pax7 and MyoD. An example image of Pax7 can be found in Figure 40. Staining intensity is very faint and we are working on protocols that will improve this. Measuring anti-Pax7 will be a valuable marker for early muscle regeneration.

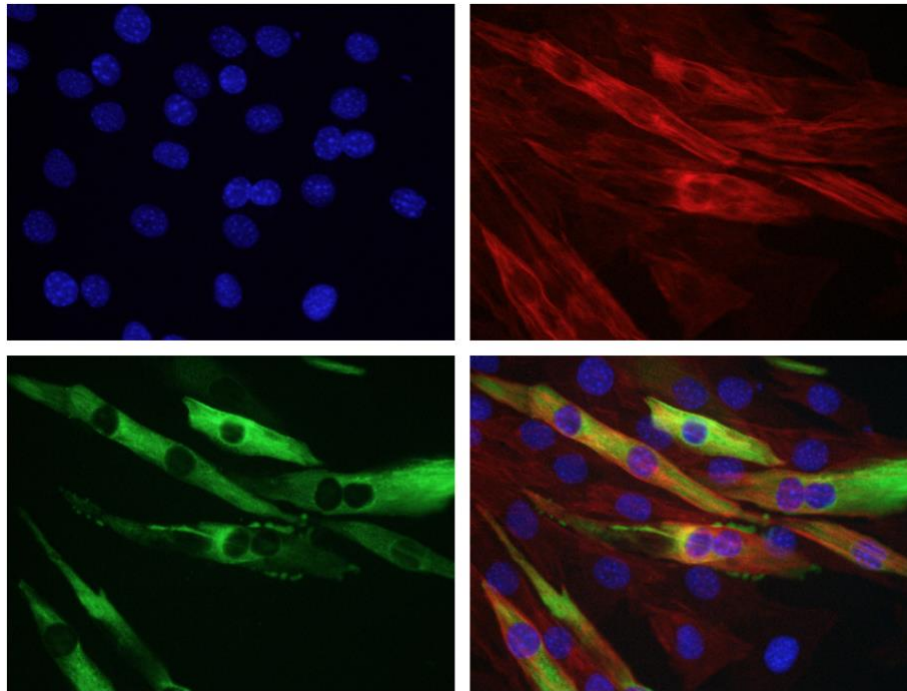


**Figure 39:** C2C12 cell culture on day 4 of differentiating in media containing 2% horse serum. Blue = DAPI, Green = MF20 (myosin marker), Red = Phalloidin (actin marker). Images taken at 40x.

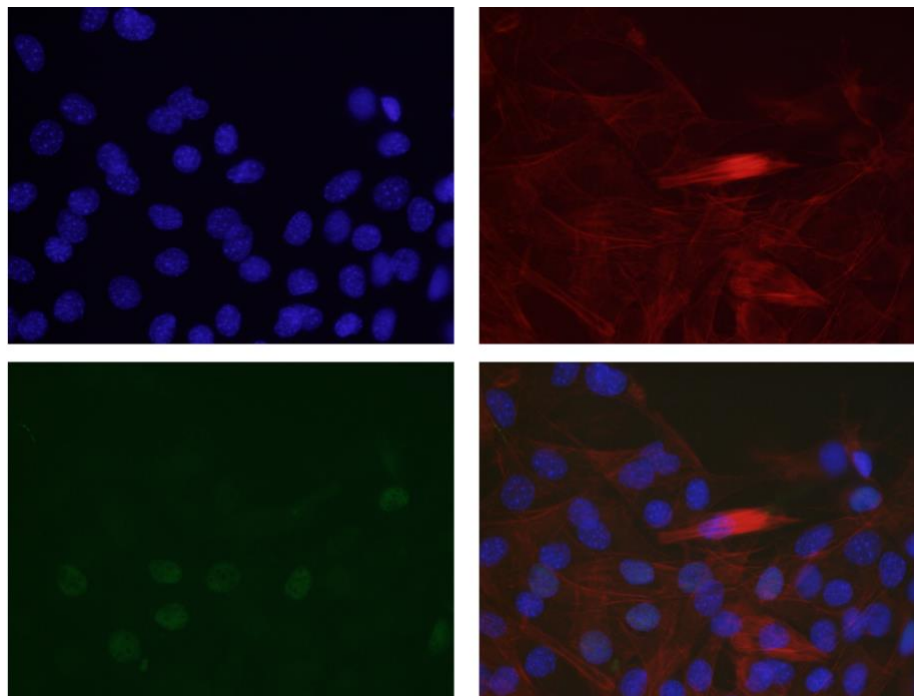


**Figure 40:** C2C12 cell culture on day 3 of differentiating in media containing 2% horse serum. In the bottom left panel, anti-Pax7 staining intensity is very faint. Blue = DAPI, Green = anti-Pax7, Red = Phalloidin (actin marker). Images taken at 40x.

In the statement of work, Specific Aim 3 was proposed with 2 major tasks. The goal of Major Task 1 was to determine whether LIV directly induces expression of pro-healing genes in

cultured Mp and EPC. The goal of Major Task 2 was to determine whether LIV directly induces functional pro-angiogenic and pro-myogenic properties of cultured Mp and EPC. Unfortunately, we ran out of time to complete these experiments within the reporting period of the grant, however we are still planning on performing them in the future.

**What opportunities for training and professional development has the project provided?**

Nothing to report

**How were the results disseminated to communities of interest?**

1. Ms. Pongkitwitoon presented data at the 2015 American Society for Bone and Mineral Research Annual Meeting on October 12, 2015 which showed that cultured macrophages are responsive to LIV by downregulating expression of pro-inflammatory markers and upregulating expression of pro-healing markers (Specific Aim 3, Major Task 1, Subtask 1 and Major Task 2, Subtask 1).
2. Mr. Corbiere gave a presentation at the Clinical and Rehabilitative Medicine Research Program (CRM RP) In-Progress Review Conference on February 5, 2016.

**What do you plan to do during the next reporting period to accomplish the goals and objectives?**

Nothing to report

#### **4. IMPACT**

**What was the impact on the development of the principal discipline(s) of the project?**

Traumatic musculoskeletal injuries are among the most common injuries experienced during military combat and recovery from these injuries is typically prolonged and incomplete, leading to impaired muscle function, joint stiffness and loss of mobility. Unfortunately, effective treatments for improving the recovery of muscle structure and function and consequent joint mobility are lacking. Our long-term goal is to develop a device and treatment protocol that provide a safe, inexpensive, and easy to apply treatment that will help to restore normal muscle and joint function to injured military personnel.

Based on our experiments, locally applied LIV is more effective than whole-body applied LIV, however both were beneficial. Parameters of 90 Hz frequency and 0.2 g acceleration were more effective than 45 Hz and 0.4 g. Muscle fibers from injured gastrocnemius muscles in mice that were exposed to LIV for 30 minutes per day, increased in size by day 14, but not day 7. Timing of LIV treatment is also important since delaying the start of treatment until day 14 did not show improvements in fiber size. Cultured macrophages were responsive to LIV signal as shown by reduced expression of pro-inflammatory genes and increased expression of pro-healing genes. Taken together, LIV shows promise as a non-invasive and simple treatment that is capable of increasing muscle growth following traumatic muscle injury by modulating genes associated with healing and inflammation. This would result in reduced joint stiffness, increased mobility, and improved quality of life in polytrauma patients

**What was the impact on other disciplines?**

Nothing to report

**What was the impact on technology transfer?**

Nothing to report

**What was the impact on society beyond science and technology?**

Nothing to report

**5. CHANGES/PROBLEMS**

**Changes in approach and reasons for change**

Nothing to report

**Actual or anticipated problems or delays and actions or plans to resolve them**

Nothing to report

**Changes that had a significant impact on expenditures**

Nothing to report

**Significant changes in use or care of human subjects, vertebrate animals, biohazards, and/or select agents**

Nothing to report

**6. PRODUCTS**

**Publications, conference papers, and presentations**

1. A paper was published in the Journal of Functional Morphology and Kinesiology (JFMK) using the data from the experiments performed as described in this grant. These data show that, compared to non-LIV control mice, myofiber cross-sectional area was larger in mice treated with two different LIV protocols (90 Hz/0.2 g and 45 Hz/0.4 g). Minimum fiber diameter was also larger in mice treated with LIV of 90 Hz/0.2 g. There was also a trend toward a reduction in collagen deposition at 45 Hz/0.4 g ( $p = 0.059$ ). These findings suggest that LIV may improve muscle healing by enhancing myofiber growth and reducing fibrosis (Specific Aim 1, Major Task 1, Subtask 3 and 4). Federal support was acknowledged within the manuscript.
  - Corbiere TF, Weinheimer-Haus EM, Judex S, Koh TJ. 2017 Dec 21. *Low Intensity Vibration improves muscle healing in a mouse model of laceration injury*. J Funct Morphol Kinesiol. Vol. 3(1). pii: 1. doi: 10.3390/jfmk3010001.
2. We published data indicating macrophages are responsive to LIV, which downregulates expression of pro-inflammatory markers and upregulates expression of pro-healing markers (Specific Aim 3, Major Task 1, Subtask 1 and Major Task 2, Subtask 1) in the Journal of Biomechanics. An abstract of these data was also submitted for presentation in the 2015

American Society for Bone and Mineral Research annual meeting and was published in the Journal of Bone and Mineral Research.

- Pongkitwitoon, S., et al., *Low-intensity vibrations accelerate proliferation and alter macrophage phenotype in vitro*. Journal of Biomechanics, 2016. **49**(5): p. 793-796.
- Pongkitwitoon, S., et al., *Low Intensity Vibrations Alter Macrophage Phenotype*. Journal of Bone and Mineral Research, 2015. **30**: Supplement 1

Nothing to report

### Technologies or techniques

Nothing to report

### Inventions, patent applications, and/or licenses

Nothing to report

### Other Products

Nothing to report

## 7. PARTICIPANTS & OTHER COLLABORATING ORGANIZATIONS

### What individuals have worked on the project?

<b>Name:</b>	Timothy Koh
<b>Project Role:</b>	PI
<b>Researcher Identifier (e.g. ORCID ID):</b>	0000-0001-6549-7060
<b>Nearest person month worked:</b>	1 academic month, 1 summer month
<b>Contribution to Project:</b>	Oversaw all aspects of the study including the in vivo LIV experiments and other activities at UIC

<b>Name:</b>	Stefan Judex
<b>Project Role:</b>	Co-I (SBU)
<b>Researcher Identifier (e.g. ORCID ID):</b>	0000-0002-4511-1535
<b>Nearest person month worked:</b>	2 summer months
<b>Contribution to Project:</b>	Oversaw in vitro experiments at SBU and worked with machine

	shop at SBU to manufacture device for local application of LIV
--	--

<b>Name:</b>	Norifumi Urao
<b>Project Role:</b>	Co-I (UIC)
<b>Researcher Identifier (e.g. ORCID ID):</b>	0000-0001-9750-8406
<b>Nearest person month worked:</b>	3 calendar months
<b>Contribution to Project:</b>	Oversaw MRI data collection and analysis.

<b>Name:</b>	Thomas Corbiere
<b>Project Role:</b>	PhD Candidate
<b>Researcher Identifier (e.g. ORCID ID):</b>	0000-0001-5408-0024
<b>Nearest person month worked:</b>	6 calendar months
<b>Contribution to Project:</b>	Performed analyses for Specific Aim 1 and performed in vivo and in vitro experiments during years 2-4.

<b>Name:</b>	Aaron Damato
<b>Project Role:</b>	Graduate Student (SBU)
<b>Researcher Identifier (e.g. ORCID ID):</b>	0000-0003-0557-0849
<b>Nearest person month worked:</b>	4 calendar months
<b>Contribution to Project:</b>	Performed in vitro experiments on macrophages for Specific Aim 3.
<b>Funding Support:</b>	Biomedical Engineering Department at SBU and National

	Aeronautics and Space Administration
--	--------------------------------------

<b>Name:</b>	Eileen Weinheimer-Haus
<b>Project Role:</b>	Post-doctoral researcher
<b>Researcher Identifier (e.g. ORCID ID):</b>	
<b>Nearest person month worked:</b>	
<b>Contribution to Project:</b>	Performed analyses for Specific Aim 1 and performed in vivo and in vitro experiments during year 1.

**Has there been a change in the active other support of the PD/PI(s) or senior/key personnel since the last reporting period?**

Nothing to report

**What other organizations were involved as partners?**

**Organization name:** Stony Brook University

**Location:** Stony Brook, New York

**Partner's contribution to the project:** Dr. Judex completed the manufacturing of a device to deliver LIV locally to injured tissue and to accomplish the tasks in Specific Aim 3. The initial in vitro experiments for Specific Aim 3 in macrophages were completed at SBU.



## Short communication

## Low-intensity vibrations accelerate proliferation and alter macrophage phenotype in vitro

Suphannee Pongkitwitoon <sup>a,1</sup>, Eileen M. Weinheimer-Haus <sup>b,1</sup>, Timothy J. Koh <sup>b</sup>, Stefan Judex <sup>a,\*</sup><sup>a</sup> Department of Biomedical Engineering, Stony Brook University, Stony Brook, NY 11794, USA<sup>b</sup> Department of Kinesiology & Nutrition, Center for Wound Healing and Tissue Regeneration, University of Illinois at Chicago, Chicago, IL 60612, USA

## ARTICLE INFO

## Article history:

Accepted 29 January 2016

## Keywords:

Mechanical signals  
Vibrations  
Macrophages  
Cell Phenotype  
In Vitro Cell Culture

## ABSTRACT

Macrophages are essential for the efficient healing of various tissues. Although many biochemical signaling pathways have been well characterized in macrophages, their sensitivity to mechanical signals is largely unexplored. Here, we applied low-intensity vibrations (LIV) to macrophages to determine whether macrophages could directly transduce LIV signals into changes in the expression of genes and proteins involved in tissue repair. Two different LIV signal frequencies (30 Hz or 100 Hz) were combined with two acceleration magnitudes (0.15g or 1g) to generate four distinct LIV signals that were applied to cultured murine macrophages. All four LIV signals significantly increased macrophage number after 3 days of stimulation with the combination of the smallest acceleration and the highest frequency (0.15g at 100 Hz) generating the largest response. Compared to non-LIV controls, gene expression of the pro-healing growth factors VEGF and TGF- $\beta$  increased with all four LIV signals (Day 1). LIV also decreased protein levels of the pro-inflammatory cytokines IL-6, IFN- $\gamma$ , and TNF- $\alpha$  (Days 1 and 3). These data demonstrate the sensitivity of macrophages to high-frequency oscillations applied at low intensities and may suggest that the benefit of LIV for tissue repair may be based on reducing inflammation and promoting a pro-healing macrophage phenotype.

© 2016 Elsevier Ltd. All rights reserved.

## 1. Introduction

Macrophages play a critical role in the healing of various tissues (Duffield et al., 2005; Lucas et al., 2010; Mirza et al., 2009; Summan et al., 2006; van Amerongen et al., 2007). Tissue repair consists of overlapping phases of inflammation, proliferation, and remodeling, and macrophages are present in all phases. As tissue repair progresses, macrophages exhibit transitions in phenotype and function, although the precise factors regulating these transitions have not been fully elucidated (Novak and Koh, 2013a, b). During efficient healing, macrophages appear to orchestrate transition from one phase to the next, contributing to phagocytosis of necrotic tissue, cell proliferation, angiogenesis, collagen deposition and matrix remodeling. However, dysregulation of macrophage function can contribute to failure to heal or fibrosis in several pathological situations (Mirza and Koh, 2011; Mirza et al.,

2013; Sindrilaru et al., 2011; Villalta et al., 2011). Thus, therapies that modulate macrophage phenotype and function may provide an avenue to promote tissue repair.

Accumulating evidence demonstrates that mechanical stimulation via low-intensity vibration (LIV;  $\leq 1g$  acceleration magnitude of the oscillating plate) can be anabolic and/or anti-catabolic in musculoskeletal tissues including bone (Garman et al., 2007; Gilsanz et al., 2006) and enhance neuromuscular control (Fu et al., 2013). LIV has also been shown to accelerate bone regeneration (Hwang et al., 2009) and skin wound healing (Weinheimer-Haus et al., 2014) but the underlying mechanism(s) remains to be elucidated. While LIV has the potential to influence many cell types involved in tissue repair, macrophages are sensitive to mechanical signals as both cyclic and static stretch, albeit at much greater magnitudes than LIV, rapidly induced gene expression in monocyte/macrophages (Wehner et al., 2010; Yang et al., 2000). Thus, the aim of this study was to determine whether macrophages could directly transduce LIV signals into changes in the expression of genes and proteins involved in tissue repair. We also tested whether LIV frequency and magnitude may play a role in modulating macrophage response.

\* Correspondence to: Stony Brook University, Bioengineering Building, Rm 213, Stony Brook, NY 11794-5281, USA. Tel.: +1 631 632 1549; fax: +1 631 632 8577.

E-mail address: [stefan.judex@stonybrook.edu](mailto:stefan.judex@stonybrook.edu) (S. Judex).

<sup>1</sup> Contributed equally.



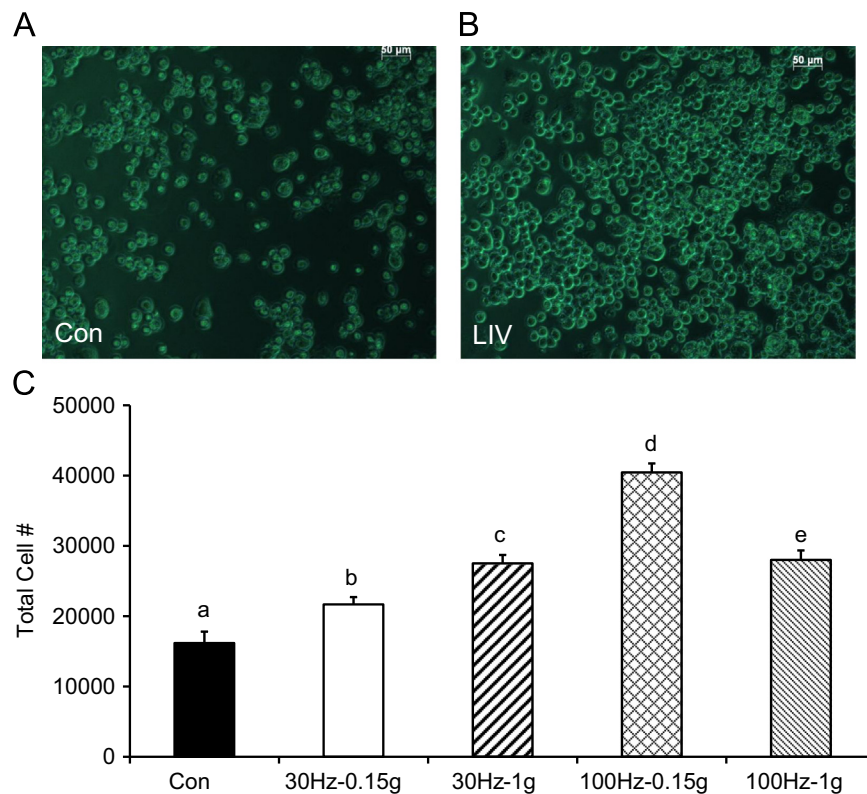


**Fig. 1.** (A and B) Representative images of cells double stained with calcein AM (green; live cells) and ethidium homodimer (red; dead cells) following exposure to (A) non-LIV sham or (B) LIV (100 Hz-0.15g) treatments. (C) Cells were exposed to one of four LIV signals or sham and cell number was determined after 3 consecutive days of stimulation. Labeled means without a common letter differ,  $p \leq 0.05$ . (For interpretation of the references to color in this figure legend, the reader is referred to the web version of this article.)

## 2. Materials and methods

### 2.1. Cell culture

Murine macrophages (J774A.1, ATCC, Manassas, VA) were cultured in RPMI 1640 (Gibco, <http://www.invitrogen.com>) supplemented with 10% heat inactivated fetal bovine serum (HI-FBS, Gibco 10082-147) and 1% penicillin/streptomycin and incubated at 37 °C, 5% CO<sub>2</sub>.

### 2.2. Mechanical stimulation

Vibration was applied horizontally as described elsewhere (Uzer et al., 2012). Briefly, cells were exposed to either a non-LIV sham control, or one of the following four signal combinations of LIV frequency and acceleration: 30 Hz and 1g, 100 Hz and 1g, 30 Hz and 0.15g, and 100 Hz and 0.15g. Vibrations were applied for 20 min/session, 2 × /day; sessions were separated by a 2 h rest period. Non-LIV control cell culture plates were handled identically to experimental plates except that vibrations were not applied.

### 2.3. Cell number

Macrophages were seeded at a density of 7500 cells/cm<sup>2</sup>. After allowing internal equilibrium for 24 h, cells were exposed to LIV or sham treatment ( $n=9$  each) on each of three consecutive days. Cell number was determined via XTT cell proliferation assay (ATCC). On Day 3 of stimulation, immediately after LIV treatment, XTT reagent was added to the samples and incubated for 3 h prior to measuring absorbance. Cell number was calculated via comparison with a standard curve. Cell viability was checked with a live/dead cell assay (Invitrogen, NY) and visualized under a microscope (Zeiss, Germany).

### 2.4. Gene expression

To determine whether macrophages can respond within hours to the application of LIV with increased transcriptional levels of two pro-healing genes, cells were plated at a density of 18,000 cells/cm<sup>2</sup>. 48 h after plating, cells were exposed

to LIV or sham treatment ( $n=9$  each). Immediately after the second LIV treatment, cells were lysed (TRIzol, Ambion, TX) and total RNA was isolated (RNeasy, Qiagen, CA). RNA concentration and quality were determined (NanoDropND-1000, Thermo Scientific, NY). cDNA was synthesized using standard protocols (High Capacity RNA to cDNA kit, Applied Biosystems, CA) and RT-PCR was performed (StepOne, Applied Biosystems) using Taqman primer (Applied Biosystems) probes for vascular endothelial growth factor (VEGF) and transforming growth factor (TGF)- $\beta$ . Relative gene expression was determined using the  $2^{-\Delta\Delta C_t}$  method with GAPDH as the endogenous control. Results were reported relative to non-vibrated control.

### 2.5. Flow cytometry

To test whether LIV induced changes in cell proliferation were accompanied by changes in protein levels of pro-inflammatory cytokines or whether LIV could decrease their production, flow cytometric analysis was performed for interleukin (IL)-6, interferon (IFN)- $\gamma$ , and tumor necrosis factor (TNF)- $\alpha$ . Cells were plated at 18,000 cells/cm<sup>2</sup> 48 h prior to the start of the experiment and were then exposed to LIV at 0.15g and 100 Hz or sham treatment ( $n=6$  each) for 3 days. The acceleration magnitude of 0.15g at a frequency of 100 Hz was selected for this experiment because this LIV combination was most effective at increasing cell number and altering VEGF expression. Immediately after the second experimental session on Day 1 or 3, cells were collected and fixed with 3.7% formaldehyde, permeabilized with 0.1% Triton, and stained with fluorescently-labeled antibodies against IL-6, IFN- $\gamma$ , or TNF- $\alpha$  (Abcam, Cambridge, UK). Live cells and dead cells were identified using calcein AM and ethidium homodimer (Invitrogen). Stained cells were analyzed by flow cytometry (FACScan, BD) and FlowJo software (Tree Star Inc. OR); percent cell populations were gated on the cells positive for these fluorescent antibodies.

### 2.6. Statistics

Data were presented as mean  $\pm$  SD. All samples were run as triplicates and statistics were computed on averages of the triplicates, preserving the sample sizes described above. Differences between groups were identified by one-way analysis of variance (ANOVA) followed by Tukey's post hoc tests (SPSS 22.0, IBM, New York, NY).  $p$ -Values of less than 0.05 were considered significant.

### 3. Results

#### 3.1. Cell number

Fluorescence microscopic images showed predominantly viable macrophages under LIV and non-LIV conditions on Day 3 (Fig. 1). Potential differences in cell morphology were not assessed quantitatively. Flow cytometric analysis revealed that the percent live macrophages were not different across LIV treated cells and non-LIV controls ( $>99.7 \pm 2\%$ ; data not shown). All four LIV signal combinations were effective in increasing cell number. Averaged across all LIV signals and compared to non-LIV controls, LIV increased cell number by 82% ( $p < 0.001$ ) on Day 3 (Fig. 1). At 30 Hz, increasing acceleration magnitude from 0.15g to 1g increased cell number whereas at 100 Hz, cell number was greater at 0.15g than at 1g. The signal combination of 0.15g at 100 Hz provided an increase in cell number that was significantly greater than for the other three LIV signals.

#### 3.2. Transcriptional changes

To assess whether macrophages can directly transduce LIV signals into changes in the expression of genes involved in tissue repair, transcriptional levels of the pro-angiogenic growth factor VEGF and the healing-associated growth factor TGF- $\beta$  were determined immediately after the second LIV treatment. Averaged across frequency signals, LIV increased ( $p < 0.001$ ) VEGF expression by 82% at 30 Hz and by 131% at 100 Hz (Fig. 2). At 30 Hz, increasing acceleration magnitude increased VEGF expression whereas, at 100 Hz, increasing acceleration magnitude reduced VEGF transcriptional levels. Similar to data on cell proliferation, the 0.15g LIV signal applied at 100 Hz provided the greatest increase in VEGF expression (156%), significantly greater ( $p < 0.001$ ) than any other LIV signal.

LIV also upregulated the expression of TGF- $\beta$  by 46% when averaged across all LIV signals (Fig. 2). The increase in TGF- $\beta$  was qualitatively similar across the four LIV signals, however, the increase was significantly greater with the 30 Hz signals than the 100 Hz signals (52% vs. 40%,  $p < 0.001$ ).

#### 3.3. Changes in protein levels

We tested whether macrophages can convert the high-frequency low-intensity mechanical signal into changes in protein levels. Using the LIV signal that was most successful in altering cell proliferation and transcriptional levels (100 Hz-0.15g), protein expression of several cytokines were measured in macrophages after treatment on Days 1 and 3 of the protocol. LIV reduced the percentage of IL-6+, IFN- $\gamma$ +, and TNF- $\alpha$ + cells on both Days 1 and 3. The reduction was

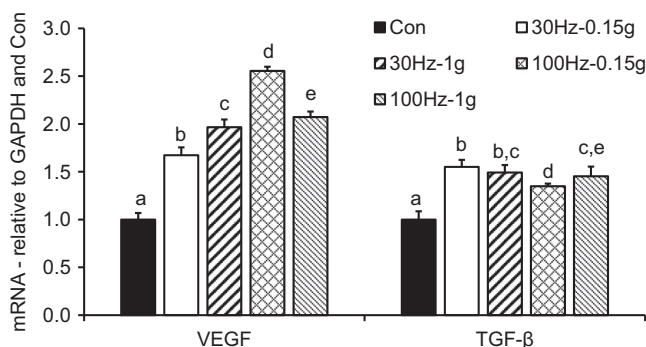


**Fig. 2.** Gene expression of pro-angiogenic growth factor VEGF and growth factor TGF- $\beta$  immediately following treatment with one of four LIV signals or non-LIV control. Labeled means without a common letter differ,  $p \leq 0.05$ .

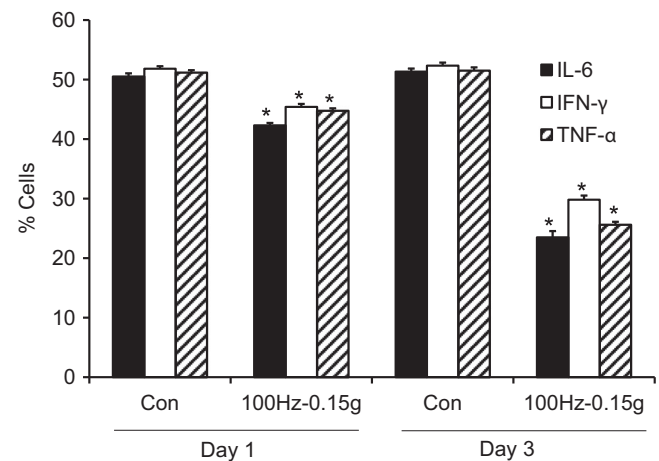


**Fig. 3.** Protein expression of pro-inflammatory cytokines IL-6, IFN- $\gamma$ , and TNF- $\alpha$  following 1 or 3 days of LIV (0.15g at 100 Hz) or sham treatment (Con). \* $p \leq 0.05$  vs. Con.

similar across the three cytokines and amounted to 12–16% on Day 1 and to 43–54% on Day 3 (Fig. 3).

### 4. Discussion

LIV may provide a novel therapeutic approach for enhancing tissue repair and has the potential to influence several cell types involved in tissue repair, including macrophages. The major finding of this study is that macrophages are sensitive to LIV and are able to transduce LIV signals into changes in cell number and in the expression of genes and proteins involved in tissue repair. Specifically, LIV increased the expression of the growth factors VEGF and TGF- $\beta$  and reduced the production of three pro-inflammatory cytokines compared to non-LIV controls. With the exception of raising TGF- $\beta$  levels, macrophages showed the greatest response to the LIV signal combination that employed the smallest amplitude at the highest frequency. Collectively these findings suggest that macrophages have the ability to differentiate between individual LIV signals based on frequency and acceleration magnitude and that the promotion of tissue repair by LIV may be mediated by changes in macrophage phenotype.

The ability of macrophages to respond to mechanical signals has been reported previously (Martin et al., 1995; Pugin et al., 1998; Wehner et al., 2010; Yang et al., 2000). In these studies, cells were stretched at magnitudes of greater than 1%, in great contrast to the oscillatory signal used here that induced deformations at least three orders of magnitude smaller (Uzer et al., 2012, 2014). In rat peritoneal macrophages, static strain of 20% induced gene expression of the pro-inflammatory genes inducible nitric oxide synthase, cyclooxygenase-2, IL-6 and IL-1 $\beta$  (Wehner et al., 2010), while cyclic strain of greater than 1% induced gene expression of the M-CSF receptor and various early response genes, which are involved in cell proliferation, differentiation and survival, in human blood monocytes/macrophages (Yang et al., 2000). In contrast to the pro-inflammatory effect of a large static stretch on rat peritoneal macrophages, we report that the dynamic extremely low magnitude LIV signal ( $<0.001\%$  deformation) had a predominantly anti-inflammatory effect on a mouse macrophage cell line. The differences in the response are likely associated with the stark differences in the mechanical signal being delivered.

During normal tissue repair, macrophages transition from a pro-inflammatory phenotype to a pro-healing phenotype. However, a sustained pro-inflammatory phenotype has been associated with impaired tissue repair (Mirza and Koh, 2011; Mirza et al., 2013; Sindrilaru et al., 2011; Villalta et al., 2011). LIV increased expression of growth factors

associated with healing and decreased expression of pro-inflammatory cytokines, indicating that LIV may promote a pro-healing macrophage phenotype. We previously reported that LIV increased VEGF levels in wounds of diabetic mice, and this was associated with increased angiogenesis and accelerated wound closure (Weinheimer-Haus et al., 2014). Perhaps, the LIV induced increase in transcriptional levels of pro-healing genes and decrease in pro-inflammatory protein levels observed here may be most beneficial in situations where sustained inflammation impairs healing (e.g., diabetes). The future exploration of precise mechanisms and pathways by which LIV can enhance healing of soft and hard (Gao et al., 2016; Hwang et al., 2009) tissues will be critical for the design of improved mechanical interventions and may also reveal novel pharmacologic targets.

It is not clear what physical parameters drive the cellular response to vibration. Using an in vitro model in which acceleration and fluid shear can be controlled independently during vibrations, we previously demonstrated that fluid shear does not regulate vibration-induced proliferation and osteogenic commitment of mesenchymal progenitor cells (Uzer et al., 2013). Instead, it is possible that cells sense LIV through an out-of-phase oscillating nucleus that converts the mechanical information to biochemical signals through inside-out signaling, in contrast to low-frequency signals like fluid flow or cellular stretch that ostensibly act through outside-in signaling (Uzer et al., 2015). The overall preference of macrophages for the 100 Hz, 0.15g signal is similar to data collected from mesenchymal progenitor cells (Uzer et al., 2013) and may suggest a similar LIV mechanotransduction mechanism for these two cell types.

The current investigation is limited in that the signaling pathways that transduce the LIV signal into cellular responses were not investigated. Another limitation is that only one time point was considered for mRNA expression and only two for protein levels. Further, it is unclear whether the observed differences in transcriptional levels, in particular TGF- $\beta$ , will translate into altered protein levels. Previous studies have indicated that multiple transduction pathways may participate in converting mechanical signals into biochemical signals, including stretch-activated ion channels, integrins, and tyrosine kinases (Banes et al., 1995; Martin et al., 1995; Takahashi et al., 1997). We previously reported that LIV increased gap junctional intracellular communication between osteocytes and this was dependent on Akt activation (Uzer et al., 2014). Future studies investigating the effects of LIV on these signaling pathways utilizing a series of time points will provide further insight into the mechanisms through which mechanical signals improve tissue repair.

In summary, we investigated the mechanosensitivity of macrophages to LIV signals in vitro. LIV increased cell number and the expression of healing-associated markers, while decreasing production of pro-inflammatory cytokines. Extrapolated, these results suggest that LIV may be beneficial for tissue repair by reducing inflammation and promoting a pro-healing macrophage phenotype in conditions such as diabetes.

## Conflict of interest statement

Stefan Judex and Timothy J. Koh have a patent pending regarding the application of vibrations for therapeutic treatment.

## Acknowledgments

We are grateful to the U.S. Department of Defense (W81XWH-14-1-0281) and the National Aeronautics and Space Administration (NNX12AL25G) for supporting this work.

## References

- Banes, A.J., Tsuzaki, M., Yamamoto, J., Fischer, T., Brigman, B., Brown, T., Miller, L., 1995. Mechanoreception at the cellular level: the detection, interpretation, and diversity of responses to mechanical signals. *Biochem. Cell Biol.* 73, 349–365.
- Duffield, J.S., Forbes, S.J., Constandinou, C.M., Clay, S., Partolina, M., Vuthoori, S., Wu, S., Lang, R., Iredale, J.P., 2005. Selective depletion of macrophages reveals distinct, opposing roles during liver injury and repair. *J. Clin. Investig.* 115, 56–65.
- Fu, C.L., Yung, S.H., Law, K.Y., Leung, K.H., Lui, P.Y., Siu, H.K., Chan, K.M., 2013. The effect of early whole-body vibration therapy on neuromuscular control after anterior cruciate ligament reconstruction: a randomized controlled trial. *Am. J. Sports Med.* 41, 804–814.
- Gao, J., Gong, H., Huang, X., Zhang, R., Ma, R., Zhu, D., 2016. Multi-level assessment of fracture calluses in rats subjected to low-magnitude high-frequency vibration with different rest periods. *Ann. Biomed. Eng.*, 1–16.
- Garman, R., Gaudette, G., Donahue, L.R., Rubin, C., Judex, S., 2007. Low-level accelerations applied in the absence of weight bearing can enhance trabecular bone formation. *J. Orthop. Res.* 25, 732–740.
- Gilsanz, V., Wren, T.A., Sanchez, M., Dorey, F., Judex, S., Rubin, C., 2006. Low-level, high-frequency mechanical signals enhance musculoskeletal development of young women with low BMD. *J. Bone Miner. Res.* 21, 1464–1474.
- Hwang, S.J., Lublinsky, S., Seo, Y.K., Kim, I.S., Judex, S., 2009. Extremely small-magnitude accelerations enhance bone regeneration: a preliminary study. *Clin. Orthop. Relat. Res.* 467, 1083–1091.
- Lucas, T., Waisman, A., Ranjan, R., Roes, J., Krieg, T., Muller, W., Roers, A., Eming, S.A., 2010. Differential roles of macrophages in diverse phases of skin repair. *J. Immunol.* 184, 3964–3977.
- Martin, D.K., Bootcov, M.R., Campbell, T.J., French, P.W., Breit, S.N., 1995. Human macrophages contain a stretch-sensitive potassium channel that is activated by adherence and cytokines. *J. Membr. Biol.* 147, 305–315.
- Mirza, R., Koh, T.J., 2011. Dysregulation of monocyte/macrophage phenotype in wounds of diabetic mice. *Cytokine* 56, 256–264.
- Mirza, R., DiPietro, L.A., Koh, T.J., 2009. Selective and specific macrophage ablation is detrimental to wound healing in mice. *Am. J. Pathol.* 175, 2454–2462.
- Mirza, R.E., Fang, M.M., Ennis, W.J., Koh, T.J., 2013. Blocking interleukin-1 $\beta$  induces a healing-associated wound macrophage phenotype and improves healing in type 2 diabetes. *Diabetes* 62, 2579–2587.
- Novak, M.L., Koh, T.J., 2013a. Macrophage phenotypes during tissue repair. *J. Leukoc. Biol.* 93, 875–881.
- Novak, M.L., Koh, T.J., 2013b. Phenotypic transitions of macrophages orchestrate tissue repair. *Am. J. Pathol.* 183, 1352–1363.
- Pugin, J., Dunn, I., Joliet, P., Tassaux, D., Magnenat, J.L., Nicod, L.P., Chevrolet, J.C., 1998. Activation of human macrophages by mechanical ventilation in vitro. *Am. J. Physiol.* 275, L1040–L1050.
- Sindrilaru, A., Peters, T., Wieschalka, S., Baican, C., Baican, A., Peter, H., Hainzl, A., Schatz, S., Qi, Y., Schlecht, A., Weiss, J.M., Wlaschek, M., Sunderkotter, C., Scharfetter-Kochanek, K., 2011. An unrestrained proinflammatory M1 macrophage population induced by iron impairs wound healing in humans and mice. *J. Clin. Investig.* 121, 985–997.
- Summan, M., Warren, G.L., Mercer, R.R., Chapman, R., Hulderman, T., Van Rooijen, N., Simeonova, P.P., 2006. Macrophages and skeletal muscle regeneration: a clodronate-containing liposome depletion study. *Am. J. Physiol. Regul. Integr. Comp. Physiol.* 290, R1488–R1495.
- Takahashi, M., Ishida, T., Traub, O., Corson, M.A., Berk, B.C., 1997. Mechanotransduction in endothelial cells: temporal signaling events in response to shear stress. *J. Vasc. Res.* 34, 212–219.
- Uzer, G., Pongkitwitoon, S., Ete Chan, M., Judex, S., 2013. Vibration induced osteogenic commitment of mesenchymal stem cells is enhanced by cytoskeletal remodeling but not fluid shear. *J. Biomech.* 46, 2296–2302.
- Uzer, G., Manske, S.L., Chan, M.E., Chiang, F.P., Rubin, C.T., Frame, M.D., Judex, S., 2012. Separating fluid shear stress from acceleration during vibrations in vitro: identification of mechanical signals modulating the cellular response. *Cell. Mol. Bioeng.* 5, 266–276.
- Uzer, G., Pongkitwitoon, S., Ian, C., Thompson, W.R., Rubin, J., Chan, M.E., Judex, S., 2014. Gap junctional communication in osteocytes is amplified by low intensity vibrations in vitro. *PLoS One* 9, e90840.
- Uzer, G., Thompson, W.R., Sen, B., Xie, Z., Yen, S.S., Miller, S., Bas, G., Styner, M., Rubin, C.T., Judex, S., Burrige, K., Rubin, J., 2015. Cell mechanosensitivity to extremely low-magnitude signals is enabled by a LINCed nucleus. *Stem Cells* 33, 2063–2076.
- van Amerongen, M.J., Harmsen, M.C., van Rooijen, N., Petersen, A.H., van Luyn, M.J., 2007. Macrophage depletion impairs wound healing and increases left ventricular remodeling after myocardial injury in mice. *Am. J. Pathol.* 170, 818–829.
- Villalta, S.A., Deng, B., Rinaldi, C., Wehling-Henricks, M., Tidball, J.G., 2011. IFN- $\gamma$  promotes muscle damage in the mdx mouse model of Duchenne muscular dystrophy by suppressing M2 macrophage activation and inhibiting muscle cell proliferation. *J. Immunol.* 187, 5419–5428.
- Wehner, S., Buchholz, B.M., Schuchtrup, S., Rocke, A., Schaefer, N., Lysson, M., Hirner, A., Kalff, J.C., 2010. Mechanical strain and TLR4 synergistically induce cell-specific inflammatory gene expression in intestinal smooth muscle cells and peritoneal macrophages. *Am. J. Physiol. Gastrointest. Liver Physiol.* 299, G1187–G1197.
- Weinheimer-Haus, E.M., Judex, S., Ennis, W.J., Koh, T.J., 2014. Low-intensity vibration improves angiogenesis and wound healing in diabetic mice. *PLoS One* 9, e91355.
- Yang, J.H., Sakamoto, H., Xu, E.C., Lee, R.T., 2000. Biomechanical regulation of human monocyte/macrophage molecular function. *Am. J. Pathol.* 156, 1797–1804.





Article

# Low-Intensity Vibration Improves Muscle Healing in a Mouse Model of Laceration Injury

Thomas F. Corbiere <sup>1,2</sup>, Eileen M. Weinheimer-Haus <sup>1,2</sup>, Stefan Judex <sup>3</sup> and Timothy J. Koh <sup>1,2,\*</sup> 

<sup>1</sup> Department of Kinesiology and Nutrition, University of Illinois at Chicago, Chicago, IL 60612, USA; tcorbi2@uic.edu (T.F.C.); eweinhei@uic.edu (E.M.W.-H.)

<sup>2</sup> Center for Wound Healing and Tissue Regeneration, University of Illinois at Chicago, Chicago, IL 60612, USA

<sup>3</sup> Department of Biomedical Engineering, Stony Brook University, Stony Brook, NY 11794, USA; stefan.judex@stonybrook.edu

\* Correspondence: tjkoh@uic.edu; Tel.: +1-312-413-9771

Received: 4 December 2017; Accepted: 15 December 2017; Published: 21 December 2017

**Abstract:** Recovery from traumatic muscle injuries is typically prolonged and incomplete, leading to impaired muscle and joint function. We sought to determine whether mechanical stimulation via whole-body low-intensity vibration (LIV) could (1) improve muscle regeneration and (2) reduce muscle fibrosis following traumatic injury. C57BL/6J mice were subjected to a laceration of the gastrocnemius muscle and were treated with LIV (0.2 g at 90 Hz or 0.4 g at 45 Hz for 30 min/day) or non-LIV sham treatment (controls) for seven or 14 days. Muscle regeneration and fibrosis were assessed in hematoxylin and eosin or Masson's trichrome stained muscle cryosections, respectively. Compared to non-LIV control mice, the myofiber cross-sectional area was larger in mice treated with each LIV protocol after 14 days of treatment. Minimum fiber diameter was also larger in mice treated with LIV of 90 Hz/0.2 g after 14 days of treatment. There was also a trend toward a reduction in collagen deposition after 14 days of treatment with 45 Hz/0.4 g ( $p = 0.059$ ). These findings suggest that LIV may improve muscle healing by enhancing myofiber growth and reducing fibrosis. The LIV-induced improvements in muscle healing suggest that LIV may represent a novel therapeutic approach for improving the healing of traumatic muscle injuries.

**Keywords:** skeletal muscle injury; laceration; low-intensity vibration; muscle regeneration; fibrosis

## 1. Introduction

Traumatic muscle injuries are among the most common injuries experienced during military combat. Approximately 70% of combat injuries involve the musculoskeletal system, many of which in recent conflicts have been caused by improvised explosive devices that cause devastating soft tissue injury [1]. Recovery is typically prolonged and incomplete and the inadequate healing response is associated with impaired muscle function, joint stiffness, and loss of mobility [2–5]. The impaired healing of traumatic muscle injuries is likely due, in part, to a disruption in blood supply and subsequent ischemia and development of fibrosis. Current therapies include anti-inflammatory strategies and physical therapy. However, we and others have demonstrated that blocking components of the inflammatory response can lead to impaired muscle healing and reduced muscle growth [4,6–11]. In addition, physical rehabilitation in the form of voluntary wheel running has resulted in modest functional improvements and increases in muscle mass associated with the upregulation of markers of fibrosis, but no hypertrophy or hyperplasia of muscle fibers after eight weeks [12]. This indicates that the improvements in function may be due to “functional fibrosis”. The lack of significant improvements in muscle function resulting from existing therapeutic approaches indicates that additional therapies are needed.

Skeletal muscle is remarkably sensitive to changes in mechanical loading. Resistance exercise and other forms of mechanical loading increase muscle mass, while reduced loading by immobilization or microgravity leads to muscle atrophy [13–15]. Mechanical stimulation via low-intensity vibration (LIV), defined as vibration with a magnitude less than 1g acceleration, can be considered a physical rehabilitation modality. Whole body mechanical stimulation via LIV has been shown to increase bone and muscle mass in growing mice and to attenuate the loss of bone and muscle during reduced loading situations [16–18]. Furthermore, LIV has been shown to accelerate bone regeneration in a cranial defect in rats [19]. With respect to tissue repair, mechanical stimulation via negative pressure therapy is commonly used to improve skin wound healing, including combat-related blast injuries [20], and we have recently shown that LIV improves the delayed healing of skin wounds in diabetic mice [21]. However, little is known about the influence of any type of mechanical stimulation on the healing of damaged muscle.

We therefore sought to determine whether mechanical stimulation via LIV could improve muscle healing following traumatic injury. We hypothesized that LIV would (1) improve muscle regeneration and (2) reduce muscle fibrosis following traumatic injury in mice. In this manuscript, we present our initial results bearing on these hypotheses.

## 2. Materials and Methods

### 2.1. Animals

C57BL/6J mice were obtained from Jackson Laboratories and housed individually in a pathogen-free, barrier facility with a 12 h light/dark cycle at a constant temperature and humidity. Experiments were performed on male mice 11–13 weeks old. Following traumatic injury of the gastrocnemius muscles, mice were randomly assigned to one of three LIV treatment groups (90 Hz, 14 days treatment;  $n = 14$  mice, 45 Hz, 14 days treatment;  $n = 18$  mice, 90 Hz 7 days treatment;  $n = 6$  mice,) or non-LIV control ( $n = 16$ ,  $n = 18$ , and  $n = 6$  mice, respectively) treatment, starting on the day of wounding. Uninjured control mice were also subjected to the LIV protocol ( $n = 3$ –5 mice). All procedures involving animals were approved by the Animal Care Committee (Protocol 17-067) at the University of Illinois at Chicago (9 June 2017).

### 2.2. Muscle Injury

Bilateral laceration of the gastrocnemius muscles was used as a model of traumatic injury and was performed as previously described [22]. Briefly, mice were anesthetized and a longitudinal incision was made through the skin on the posterior hindlimb. A scalpel was used to lacerate the lateral gastrocnemius transversely at its widest point, from the central neurovascular complex (taking care to preserve its integrity) to the lateral edge of the muscle, which is approximately 4 mm. The laceration goes through the entire thickness of the mid-belly of the muscle which is approximately 2–3 mm thick. The skin was closed, and the procedure was repeated on the contralateral leg. Muscles from injured and non-injured control mice were harvested at the indicated time points.

### 2.3. Whole Body Low-Intensity Vibration

For LIV, mice were placed in an empty cage directly on the vibrating plate and LIV was applied vertically at either 90 Hz with a peak acceleration of 0.2 g or 45 Hz with a peak acceleration of 0.4 g for 30 min per day for either seven or 14 days (Figure 1) [21]. Non-vibrated controls were placed in a separate empty cage but were not subjected to LIV. The mechanical signals were calibrated using an accelerometer attached to the inside surface of the bottom of the cage, so that the signals produced were indeed those transmitted to the feet of the mice. In addition, the amplitude of the vibrations ( $<100 \mu\text{m}$ ) were small enough that the cage did not move relative to the plate and the vibrations of the plate and the cage were in sync. The protocols used for this study were chosen based on their ability to induce positive biological effects in animals. The 90 Hz/0.2 g protocol has been used to ameliorate

bone loss in rodents [23]. The 45 Hz/0.4 g protocol has been used to accelerate bone regeneration in a cranial defect and improve wound healing in rodents [19,21].

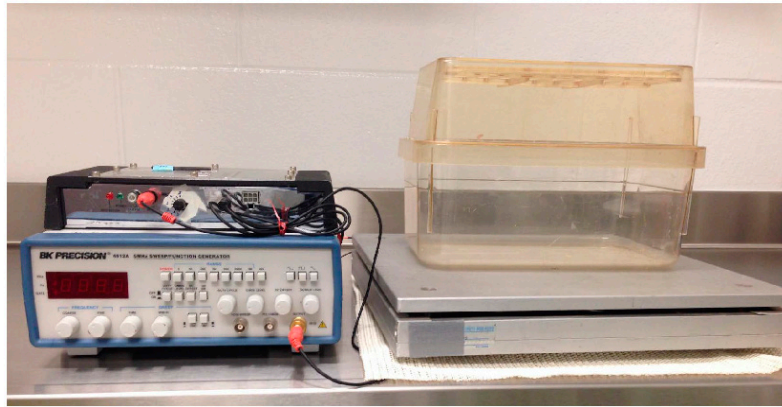


**Figure 1.** Equipment used to deliver whole-body low-intensity vibration (LIV) to mice. Mice were placed in an empty cage directly on the vibrating plate, and LIV was applied vertically at either 45 Hz or 90 Hz with a peak acceleration of either 0.4 g or 0.2 g for 30 min/day. The non-vibrated controls were similarly placed in a separate empty cage but were not subjected to LIV.

#### 2.4. Histology

Muscle regeneration and fibrosis were assessed by histological analysis, as previously described [22]. Gastrocnemius muscles were harvested, embedded in freezing medium, and flash frozen in 2-methylbutane cooled on dry ice. Serial transverse 10  $\mu$ m-thick cryosections were taken throughout the entire injured portion of the muscle. Sections with the greatest percentage of damaged, non-regenerated area were then selected for further analysis by staining with hematoxylin and eosin and Masson's trichrome, as well as immunohistochemistry.

Regeneration was quantified in hematoxylin and eosin-stained sections by morphological analysis on five representative images of each muscle section obtained using a Nikon Instruments Eclipse 80i microscope with a 40 $\times$  objective, a DS-Fi1 digital camera, and NIS Elements software (Nikon, Melville, NY, USA). Images were taken within the muscle belly and care was taken to avoid extramuscular connective tissue. Fibers were identified as either centrally-nucleated or peripherally-nucleated with no evidence of damage. Centrally-nucleated fibers likely represent both fibers that have undergone denervation and those in the process of regeneration [24]. Percent of total fibers that were classified as centrally- or peripherally-nucleated were then quantified using ImageJ (NIH, Bethesda, MD, USA). The damaged area was quantified by subtracting the area of all fibers from the total area within the field of view.

Collagen accumulation was quantified using Masson's trichrome staining. Three to six 20 $\times$  images were taken of the injured site in each muscle using a 20 $\times$  objective on an Eclipse 80i microscope with DS-Fi1 camera and NIS-Elements BR software. Masson's trichrome stains muscle fibers red, nuclei black, and collagen blue. Collagen accumulation was quantified as the percent of the total image area stained blue.

Platelet endothelial cell adhesion molecule-1 (PECAM-1), a marker for angiogenesis, was identified using anti-mouse CD31 antibody (clone 390; 1:100 in PBS; BioLegend, Inc., San Diego, CA, USA); whereas macrophage accumulation was assessed using an anti-mouse F4/80 antibody (clone BM8; 1:100 in PBS; eBioscience, Inc., San Diego, CA, USA). Slides serving as negative controls received PBS instead of primary antibody. Briefly, sections were air-dried, fixed in cold acetone, washed with PBS, quenched with 0.3% hydrogen peroxide, and washed with PBS. Sections were blocked with buffer containing 3% bovine serum albumin and then incubated with primary antibody

for 1 h at room temperature and then overnight at 4 °C. Sections were washed in PBS and incubated with biotinylated mouse adsorbed anti-rat IgG (1:200 in PBS; Vector Laboratories Inc., Burlingame, CA, USA), followed by avidin D horseradish peroxidase (1:1000 in PBS). Sections were then developed with 3,3'-diaminobenzidine (ImmPACT DAB, Cat. No. SK-4105; Vector). Three to six 20× images were taken of the injured site in each muscle using a 20× objective on an Eclipse 80i microscope with DS-Fi1 camera and NIS-Elements BR software. Angiogenesis and macrophage accumulation were quantified as the percent of the total image area stained using ImageJ (NIH).

### 2.5. Statistics

Values are reported as means  $\pm$  standard error. Data were tested for homoscedasticity and those passed were compared using two-sided *t* tests and those that did not pass were compared using the nonparametric Mann-Whitney test. Differences between groups were considered significant if  $p \leq 0.05$ . Graphpad Prism Version 7.00 (Graphpad Software, Inc, San Diego, CA, USA) was used to generate all figures.

## 3. Results

### 3.1. LIV Protocol Using 90 Hz and 0.2 g for 14 Day Treatment Period

Body mass ( $27.3 \pm 1.3$  g vs.  $27.1 \pm 1.1$  g;  $p > 0.05$ ) was not different between LIV and non-LIV groups, suggesting that mice tolerated the LIV protocol well. Consistent with our hypothesis, LIV treatment at 90 Hz/0.2 g improved the healing of lacerated gastrocnemius muscle at day 14 post-injury (Figure 2A,B). Compared to non-LIV but injured control mice, both the minimum fiber diameter and the cross-sectional area of individual myofibers were significantly larger in mice treated with LIV at 14 days post-injury (Figure 2C,D). When centrally-nucleated and peripherally-nucleated myofibers were assessed separately, the minimum fiber diameters of both were significantly larger in LIV treated mice (Figure 2E), whereas cross-sectional area showed only a trend in this direction (Figure 2F). In contrast to the increase in muscle fiber size, the percent area occupied by centrally-nucleated myofibers and peripherally-nucleated myofibers was not different between LIV-treated and non-LIV control mice; however, there may be a trend towards a decrease in damaged area with LIV ( $p = 0.198$ ) (Figure 2G).

### 3.2. LIV Protocol Using 45 Hz and 0.4 g for 14 Day Treatment Period

LIV treatments at 45 Hz/0.4 g also improved the healing of lacerated gastrocnemius muscle (Figure 3A,B). Compared to non-LIV but injured control mice, the cross-sectional area but not the minimum fiber diameter of individual myofibers was larger in mice treated with LIV at 14 days post-injury (Figure 3C,D). When centrally-nucleated and peripherally-nucleated myofibers were assessed separately, the cross-sectional area of both but not the minimum fiber diameter was significantly larger in LIV treated mice (Figure 3E,F). There was no significant difference in the percent area occupied by centrally-nucleated myofibers or damaged area between LIV-treated and non-LIV control mice; however, there may be a trend towards an increase in percent area of peripherally-nucleated fibers with LIV ( $p = 0.2$ ) (Figure 3G). Considering the increases in fiber diameter and/or area between each of the LIV protocols, these morphological data suggest that LIV may not influence the formation of regenerating fibers, but instead enhances myofiber growth after formation.

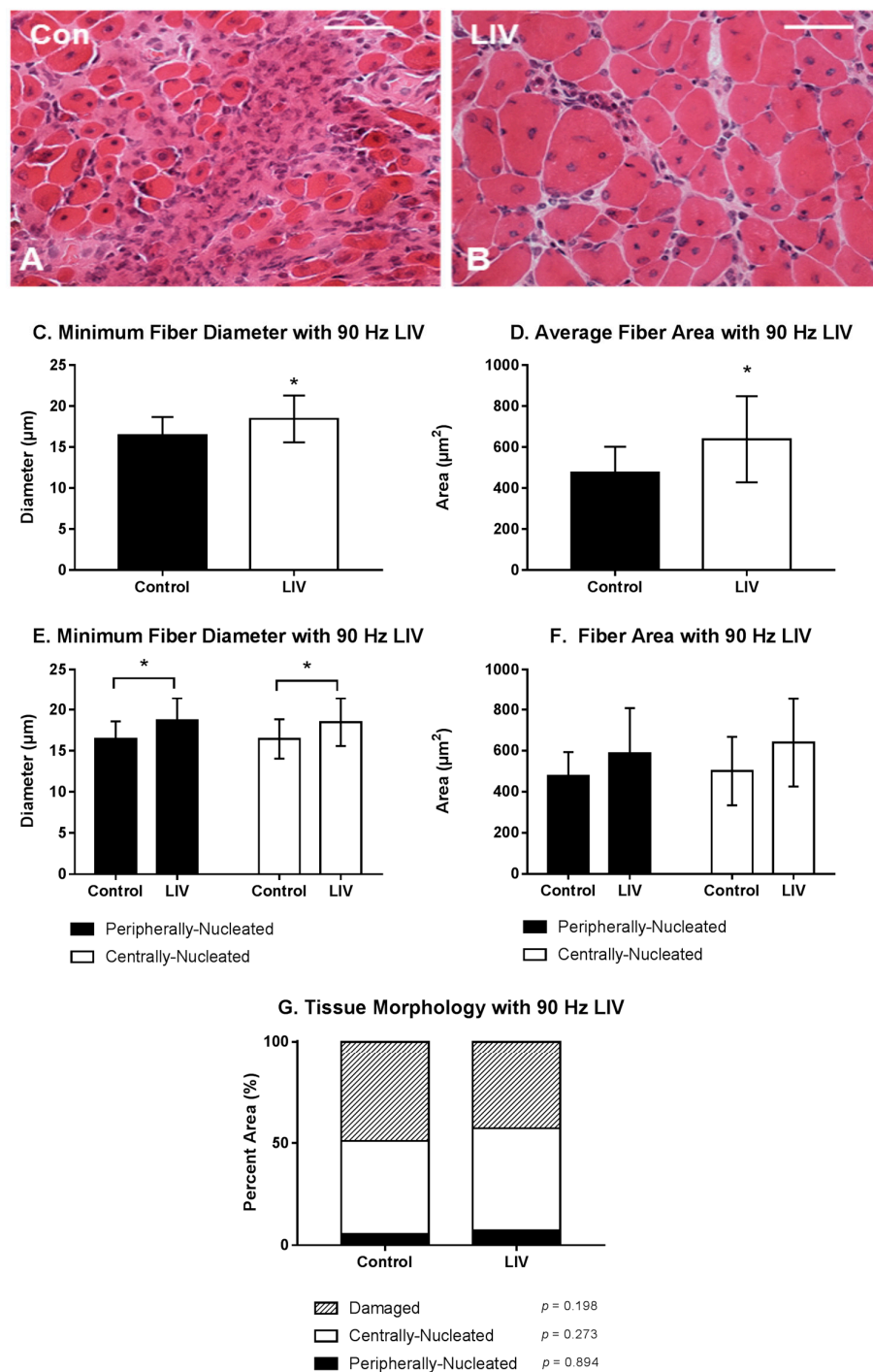


**Figure 2.** Low-intensity vibration (LIV) at 90 Hz and 0.2 g enhances myofiber growth at day 14 post-injury following laceration muscle injury in mice. Gastrocnemius muscles were lacerated and collected for histological analysis at day 14 post-injury. (A,B) Representative images of hematoxylin and eosin-stained sections (scale bar = 50  $\mu\text{m}$ , 40 $\times$  magnification); (C,E) Average minimum myofiber diameter; (D,F) average cross-sectional area of individual myofibers, and (G) percent area of injury that consists of peripherally-nucleated fibers, centrally-nucleated fibers, or damaged tissue was quantified in five 40 $\times$  fields per muscle in hematoxylin and eosin-stained sections. (C,D) All fiber types averaged together; (E,F) Myofibers grouped by type. Data are presented as mean  $\pm$  SE. \*  $p \leq 0.05$ .



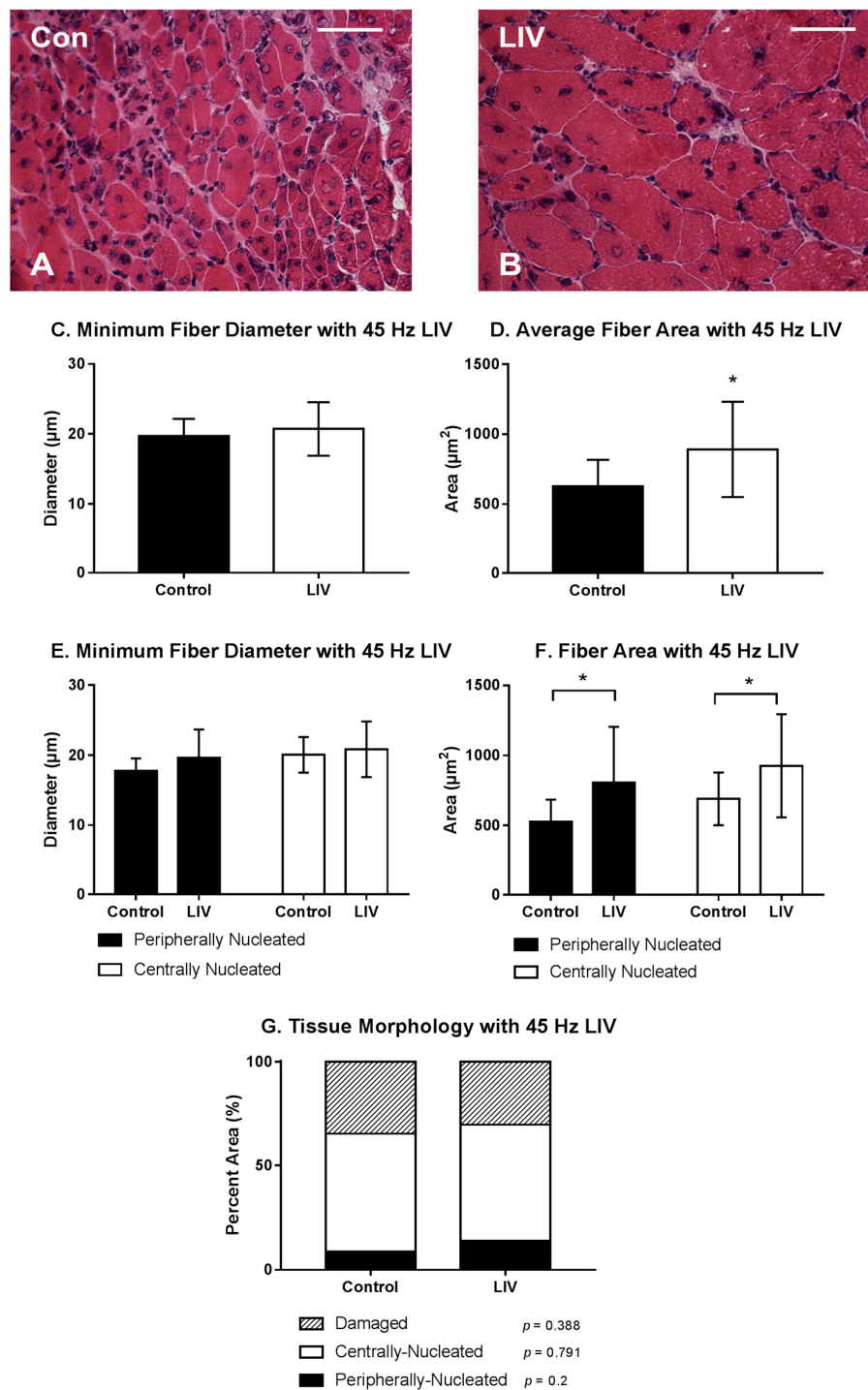


**Figure 3.** Low-intensity vibration (LIV) at 45 Hz and 0.4 g enhances myofiber growth following laceration muscle injury in mice at 14 days post-injury. Gastrocnemius muscles were lacerated and collected for histological analysis at day 14 post-injury. (A,B) Representative images of hematoxylin and eosin-stained sections (scale bar = 50  $\mu\text{m}$ , 40 $\times$  magnification); (C,E) Average minimum myofiber diameter; (D,F) average cross-sectional area of individual myofibers, and (G) percent area of injury that consists of peripherally-nucleated fibers, centrally-nucleated fibers, or damaged tissue was quantified in five 40 $\times$  fields per muscle in hematoxylin and eosin-stained sections; (C,D) All fiber types averaged together; (E,F) Myofibers grouped by type. Data are presented as mean  $\pm$  SE. \*  $p \leq 0.05$ .

### 3.3. Effects of LIV on Fibrosis for 14 Day Treatment Period

Since lacerated gastrocnemius muscle heals by a combination of regeneration and fibrosis, we also assessed the effects of LIV on muscle fibrosis. Trichrome staining in muscle cryosections revealed a trend of reduced collagen deposition in mice treated with 45 Hz/0.4 g LIV vs. non-LIV controls on day 14 following injury. This same effect was not replicated with the 90 Hz/0.2 g LIV protocol (Figure 4A–C). When considered alongside the LIV-induced increase in myofiber cross-sectional area, these findings suggest that LIV, at least the 45 Hz protocol, may improve muscle healing by enhancing myofiber growth and reducing fibrosis.

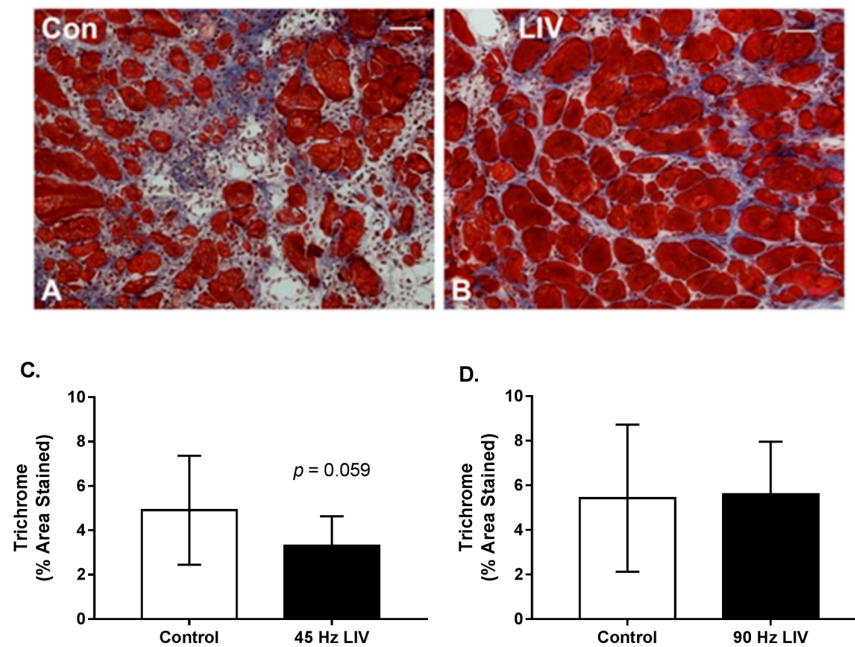


**Figure 4.** Fibrosis may be reduced in lacerated muscle following low-intensity vibration. (A,B) Representative images of trichrome-stained sections at day 14 following laceration of the gastrocnemius muscles (scale bar = 50  $\mu$ m, 20 $\times$  magnification); (C,D) Collagen accumulation was quantified as percent blue pixels in three to six 20 $\times$  fields per muscle in Masson's trichrome-stained sections. Data are presented as mean  $\pm$  SE. \*  $p \leq 0.05$ .

### 3.4. LIV Protocol Using 90 Hz and 0.2 g for Seven Day Treatment Period

Since LIV increased muscle fiber size and tended to reduce fibrosis after 14 days of treatment (Figures 2–4), the experiment was repeated and muscles were harvested at day seven to determine whether LIV induces early improvements in muscle regeneration. After seven days of treatment, LIV at 90 Hz/0.2 g did not noticeably improve the healing of lacerated gastrocnemius muscle (Figure 5A,B). Compared to non-LIV but injured control mice, both the minimum fiber diameter and the cross-sectional area of individual myofibers were not different in mice treated with LIV at 90 Hz/0.2 g on day seven post-injury (Figure 5C,D). When centrally-nucleated and peripherally-nucleated myofibers were assessed separately, neither minimum fiber diameter, fiber area, nor morphological characteristics were different between treatment groups (Figure 5E–G). Additionally, no differences were found in markers for angiogenesis or macrophage accumulation, as assessed histologically by staining with CD31 and F4/80, respectively (Figure 6). Taken together, these data indicate that LIV does not influence the early regenerative phase of healing and instead improves healing through an influence on the remodeling phase. Alternatively, seven days of LIV treatment may not be sufficient to induce observable improvements in the healing process.

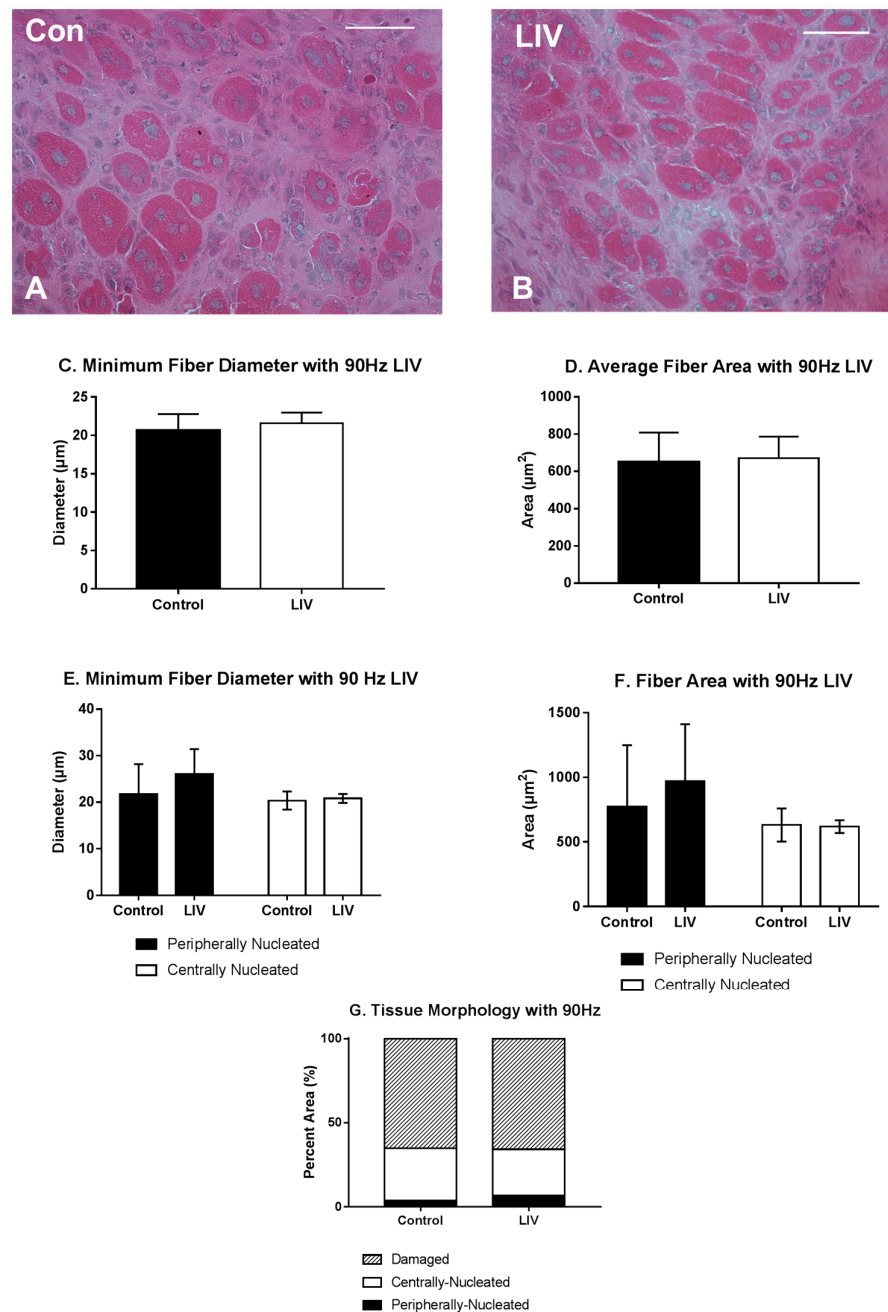


**Figure 5.** Low-intensity vibration (LIV) at 90 Hz and 0.2 g does not influence muscle regeneration on day seven post-injury following laceration muscle injury in mice. Gastrocnemius muscles were lacerated and collected for histological analysis at day seven post-injury. (A,B) Representative images of hematoxylin and eosin-stained sections (scale bar = 50  $\mu\text{m}$ , 40 $\times$  magnification); (C,E) Average minimum myofiber diameter; (D,F) average cross-sectional area of individual myofibers, and (G) percent area of injury that consists of peripherally-nucleated fibers, centrally-nucleated fibers, or damaged tissue was quantified in five 40 $\times$  fields per muscle in hematoxylin and eosin-stained sections; (C,D) All fiber types averaged together; (E,F) Myofibers grouped by type. Data are presented as mean  $\pm$  SE.



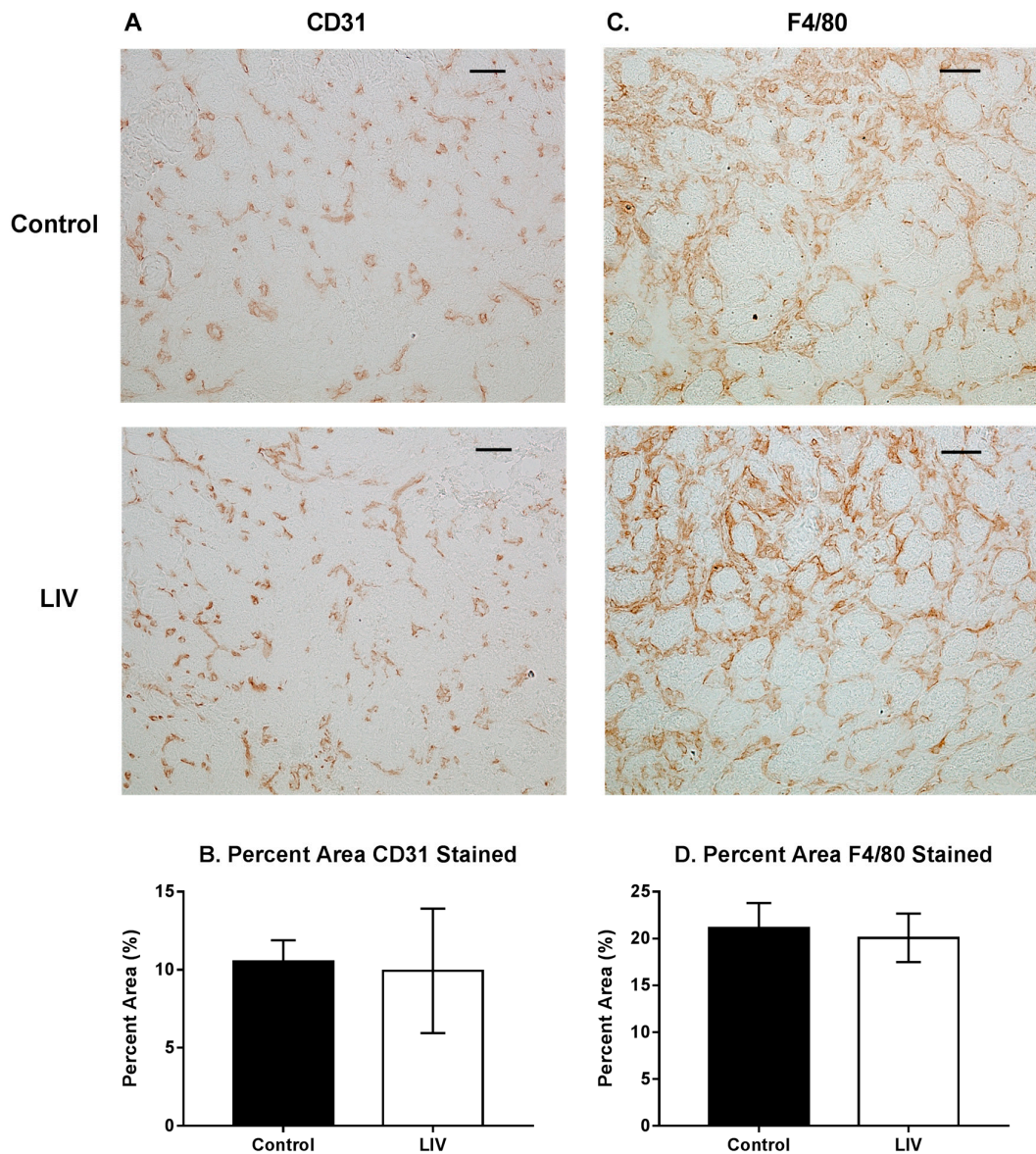


**Figure 6.** Effects of low-intensity vibration (LIV) at 90 Hz and 0.2 g on angiogenesis (CD31) and macrophage accumulation (F4/80) at day seven post-injury following laceration muscle injury in mice. Gastrocnemius muscles were lacerated and collected for histological analysis at day seven post-injury. (A) Representative images of CD31-stained sections (scale bar = 50  $\mu$ m, 20 $\times$  magnification); (B) Percent area that stained positive for CD31; (C) Representative images of F4/80-stained sections (scale bar = 50  $\mu$ m, 20 $\times$  magnification); (D) Percent area that stained positive for F4/80. Data are presented as mean  $\pm$  SE.  $n = 6$  per group.

### 3.5. Effects of LIV on Uninjured Muscle

Interestingly, in uninjured mice, LIV did not increase the average myofiber cross-sectional area after 20 days of LIV treatments, suggesting that the beneficial effects of this LIV protocol do not accrue to non-injured skeletal muscle, but likely require prior muscle damage and subsequent regeneration (Figure 7).

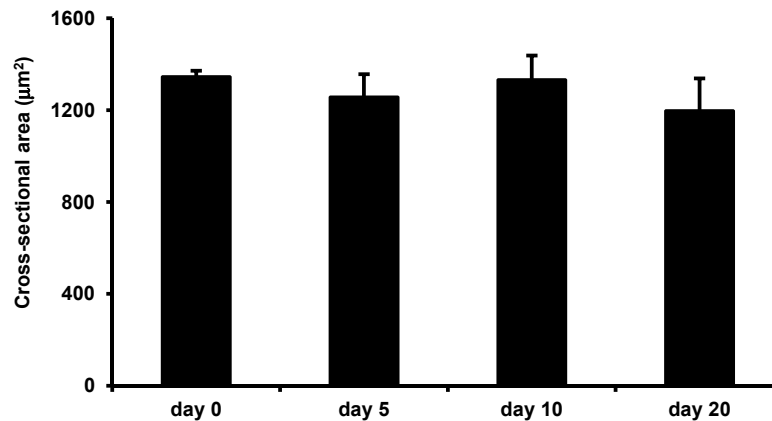


**Figure 7.** Low-intensity vibration does not enhance myofiber size in uninjured mice. Uninjured control mice were subjected to the LIV protocol and gastrocnemius muscles were collected at the indicated time points. Average cross-sectional area of individual myofibers was quantified in five 40× fields per muscle in hematoxylin and eosin-stained sections. Data are presented as mean ± SE.

#### 4. Discussion

Unlike toxin- or exercise-induced muscle injuries, recovery from traumatic muscle injuries is typically prolonged and incomplete [1,25,26], resulting in permanent impairments of muscle and joint function [2–5]. This impaired healing results in significant costs for rehabilitation, loss of time for work, and reduced combat readiness in military personnel [25]. Thus, effective therapies for promoting the healing of traumatic muscle injuries are needed. Interestingly, mechanical stimulation via LIV has been shown to ameliorate bone loss and to enhance bone regeneration [16–19]. Furthermore, we have recently shown that LIV improves the delayed healing of skin wounds in diabetic mice [21]. However, little is known about the effects of LIV on the healing of damaged muscle. We therefore determined whether mechanical stimulation via LIV could (1) improve muscle regeneration and (2) reduce muscle fibrosis following traumatic injury in mice. Our findings provide evidence that LIV indeed improves muscle repair by influencing the remodeling phase of healing.

To our knowledge, this is the first study to assess the effects of mechanical stimulation via LIV on muscle healing. We observed a larger myofiber size in mice that received LIV treatment protocols at 90 Hz/0.2 g or 45 Hz/0.4 g for 14 days post-injury, but not for seven days post-injury, compared to non-LIV controls. LIV did not promote myofiber hypertrophy after 20 days of LIV treatments in uninjured mice. These findings indicate that prior muscle damage and subsequent regeneration is likely required for the beneficial effects of LIV. While the pathways that modulate the cellular response to LIV remain to be elucidated, we can speculate that LIV may exert local and/or systemic effects and that these effects are likely at later stages of healing since improvements were not seen until 14 days post-injury. LIV may increase fiber size via direct mechanical effects on muscle cells, since muscle is particularly sensitive to mechanical stimuli, or indirectly via the production of cytokines and growth factors that promote muscle growth. Alternatively, it is well documented that LIV can be anabolic to bone, and thus, LIV may promote the mobilization and/or homing of bone marrow-derived cells to the injured tissue. These cells include progenitor cells and monocytes/macrophages, which are important during tissue repair as they release growth factors and cytokines that promote tissue healing [6,7,10,27]. Our findings suggest that LIV may have anabolic effects on regenerating muscle and the elucidating mechanisms underlying the local and/or systemic effects of LIV warrant further investigation.

The development of fibrosis likely contributes to the impaired healing of traumatic muscle injuries. As such, experimental therapeutic approaches have attempted to improve healing by blocking actions of transforming growth factor (TGF)-β1 and the associated fibrosis; these anti-fibrotic agents have included suramin, interferon (IFN)-γ, decorin, and losartan [28–31]. While these agents have shown

promise in animal studies in reducing fibrosis and improving regeneration following traumatic muscle injury, many of these agents have serious side effects and would likely not be an option for treating muscle injuries. In the current study, the trend of reduced collagen deposition following injury in the LIV-treated mice at 14 days post-injury with the 45 Hz protocol suggests that LIV may serve as a safe, non-pharmacological therapy for reducing fibrosis. Because LIV was initiated within hours of the injury, our findings suggest that LIV may be effective in attenuating or preventing fibrosis. Whether or not LIV can reverse fibrosis after it has been established warrants further investigation.

One reason that healing is impaired in models of traumatic injury (such as laceration) compared to other injury models (such as toxin-induced injury) may be the disruption of blood supply to the muscle. Thus, improving the perfusion of damaged muscle may be an additional mechanism by which LIV can improve healing. Although LIV did not improve CD31 staining, a marker for angiogenesis, at day seven in the current study, we have recently shown that LIV improves the delayed healing of skin wounds in diabetic mice, which was associated with an increase in CD31 staining [21]. LIV can also acutely increase blood flow in the skin of the ear of hairless mice, the skin of the dorsal side of the lower leg of healthy human subjects, and the skin of the underside of the forearm of both healthy and Type 2 diabetic human subjects [32–34]. Furthermore, nitric oxide (NO) is well-known for its vasodilatory effects. Serum nitrite levels, a marker for NO signaling, increases with the application of LIV in juvenile pigs [35,36]. L-NAME, an NO synthase inhibitor, blocked the LIV induced increase in skin blood flow in the ear of hairless mice [32,35,36]. LIV has been shown to improve the healing of pressure ulcers in humans by upregulating NO and improving blood supply [37]. Relatedly, LIV also slowed the progression of pressure ulcers into deep tissue injury in a rat model [38]. Thus, future studies should further investigate the influence of LIV on blood vessel formation and the perfusion of damaged skeletal muscle.

Our study is limited in that the effects of LIV on muscle healing were only assessed at two time points. Skeletal muscle repair following injury occurs in four overlapping phases: hemostasis, inflammation, new muscle fiber formation, and subsequent remodeling. Our findings are likely relevant to the remodeling phase as we have previously shown that new myofiber formation predominates during the first two weeks following muscle laceration, while myofiber maturation and collagen deposition typically occur thereafter [22]. We are currently performing a time course study that investigates the effect of LIV on muscle healing during each of the different phases of healing. This study is also limited in that mechanisms underlying LIV-induced improvements in healing were not thoroughly investigated. The purposes of this initial study were to evaluate whether or not whole-body LIV could be a feasible and effective strategy for improving the healing of a traumatic muscle injury and whether varying LIV parameters (frequency and amplitude) had an impact on improving the healing of a traumatic muscle injury. Further optimization of the LIV protocol may yield even better results. Now that we have established LIV as a potential therapeutic strategy for muscle healing, mechanistic studies are ongoing. Finally, this study is limited by the lack of assessment of muscle functional recovery. We plan to determine the effect of LIV on the time course of functional recovery in a future study.

In summary, our findings are consistent with our hypothesis that LIV improves muscle regeneration and reduces fibrosis following traumatic injury. Thus, LIV may provide a novel, non-pharmacological therapeutic approach for improving the prolonged and incomplete healing typically seen with these injuries. The LIV protocol used in this study is simple, inexpensive, and safe; at the amplitude employed (<100  $\mu$ m), the vibration is barely perceptible to human touch. Furthermore, the LIV protocol could be easily translated to use for human studies, since the equipment utilized has already been used to ameliorate bone loss in human subjects [17,39–42].

**Acknowledgments:** The institution of one or more of the authors has received funding from the Department of Defense (W81XWH-14-1-0281 to Timothy J. Koh and Stefan Judex) and the National Institutes of Health (EB01435101A to Stefan Judex. and T32DE018381 to Eileen M. Weinheimer-Haus).

**Author Contributions:** Timothy J. Koh and Stefan Judex conceived and designed the experiments; Thomas F. Corbiere and E.M.W.-H. performed the experiments; Thomas F. Corbiere, Eileen M. Weinheimer-Haus, Timothy J. Koh, and Stefan Judex analyzed the data; Thomas F. Corbiere, Eileen M. Weinheimer-Haus, Timothy J. Koh, and Stefan Judex wrote the paper.

**Conflicts of Interest:** Timothy J. Koh and Stefan Judex have a patent pending regarding the application of vibrations for therapeutic treatment. Eileen M. Weinheimer-Haus and Thomas F. Corbiere certify that he or she, or a member of his or her immediate family, has no funding or commercial associations (e.g., consultancies, stock ownership, equity interest, patent/licensing arrangements, etc.) that might pose a conflict of interest in connection with the submitted article.

## References

1. Covey, D.C. Combat orthopaedics: A view from the trenches. *J. Am. Acad. Orthop. Surg.* **2006**, *14*, S10–S17. [[CrossRef](#)] [[PubMed](#)]
2. Bedair, H.; Liu, T.T.; Kaar, J.L.; Badlani, S.; Russell, A.J.; Li, Y.; Huard, J. Matrix metalloproteinase-1 therapy improves muscle healing. *J. Appl. Physiol.* **2007**, *102*, 2338–2345. [[CrossRef](#)] [[PubMed](#)]
3. Menetrey, J.; Kasemkijwattana, C.; Fu, F.H.; Moreland, M.S.; Huard, J. Suturing versus immobilization of a muscle laceration. A morphological and functional study in a mouse model. *Am. J. Sports Med.* **1999**, *27*, 222–229. [[CrossRef](#)] [[PubMed](#)]
4. Shen, W.; Li, Y.; Tang, Y.; Cummins, J.; Huard, J. NS-398, a cyclooxygenase-2-specific inhibitor, delays skeletal muscle healing by decreasing regeneration and promoting fibrosis. *Am. J. Pathol.* **2005**, *167*, 1105–1117. [[CrossRef](#)]
5. Vaittinen, S.; Hurme, T.; Rantanen, J.; Kalimo, H. Transected myofibres may remain permanently divided in two parts. *Neuromuscul. Disord. NMD* **2002**, *12*, 584–587. [[CrossRef](#)]
6. Arnold, L.; Henry, A.; Poron, F.; Baba-Amer, Y.; van Rooijen, N.; Plonquet, A.; Gherardi, R.K.; Chazaud, B. Inflammatory monocytes recruited after skeletal muscle injury switch into antiinflammatory macrophages to support myogenesis. *J. Exp. Med.* **2007**, *204*, 1057–1069. [[CrossRef](#)] [[PubMed](#)]
7. Bryer, S.C.; Fantuzzi, G.; van Rooijen, N.; Koh, T.J. Urokinase-type plasminogen activator plays essential roles in macrophage chemotaxis and skeletal muscle regeneration. *J. Immunol.* **2008**, *180*, 1179–1188. [[CrossRef](#)] [[PubMed](#)]
8. DiPasquale, D.M.; Cheng, M.; Billich, W.; Huang, S.A.; van Rooijen, N.; Hornberger, T.A.; Koh, T.J. Urokinase-type plasminogen activator and macrophages are required for skeletal muscle hypertrophy in mice. *Am. J. Physiol. Cell Physiol.* **2007**, *293*, C1278–C1285. [[CrossRef](#)] [[PubMed](#)]
9. Novak, M.L.; Billich, W.; Smith, S.M.; Sukhija, K.B.; McLoughlin, T.J.; Hornberger, T.A.; Koh, T.J. COX-2 inhibitor reduces skeletal muscle hypertrophy in mice. *Am. J. Physiol. Regul. Integr. Comp. Physiol.* **2009**, *296*, R1132–R1139. [[CrossRef](#)] [[PubMed](#)]
10. Novak, M.L.; Bryer, S.C.; Cheng, M.; Nguyen, M.H.; Conley, K.L.; Cunningham, A.K.; Xue, B.; Sisson, T.H.; You, J.S.; Hornberger, T.A.; et al. Macrophage-specific expression of urokinase-type plasminogen activator promotes skeletal muscle regeneration. *J. Immunol.* **2011**, *187*, 1448–1457. [[CrossRef](#)] [[PubMed](#)]
11. Summan, M.; Warren, G.L.; Mercer, R.R.; Chapman, R.; Hulderman, T.; Van Rooijen, N.; Simeonova, P.P. Macrophages and skeletal muscle regeneration: A clodronate-containing liposome depletion study. *Am. J. Physiol. Regul. Integr. Comp. Physiol.* **2006**, *290*, R1488–R1495. [[CrossRef](#)] [[PubMed](#)]
12. Aurora, A.; Garg, K.; Corona, B.T.; Walters, T.J. Physical rehabilitation improves muscle function following volumetric muscle loss injury. *BMC Sports Sci. Med. Rehabil.* **2014**, *6*, 41. [[CrossRef](#)] [[PubMed](#)]
13. Marimuthu, K.; Murton, A.J.; Greenhaff, P.L. Mechanisms regulating muscle mass during disuse atrophy and rehabilitation in humans. *J. Appl. Physiol.* **2011**, *110*, 555–560. [[CrossRef](#)] [[PubMed](#)]
14. Russell, A.P. Molecular regulation of skeletal muscle mass. *Clin. Exp. Pharmacol. Physiol.* **2010**, *37*, 378–384. [[CrossRef](#)] [[PubMed](#)]
15. Spangenburg, E.E. Changes in muscle mass with mechanical load: Possible cellular mechanisms. *Appl. Physiol. Nutr. Metab. Physiol. Appl. Nutr. Metab.* **2009**, *34*, 328–335. [[CrossRef](#)] [[PubMed](#)]
16. Garman, R.; Gaudette, G.; Donahue, L.R.; Rubin, C.; Judex, S. Low-level accelerations applied in the absence of weight bearing can enhance trabecular bone formation. *J. Orthop. Res.* **2007**, *25*, 732–740. [[CrossRef](#)] [[PubMed](#)]



17. Gilsanz, V.; Wren, T.A.; Sanchez, M.; Dorey, F.; Judex, S.; Rubin, C. Low-level, high-frequency mechanical signals enhance musculoskeletal development of young women with low BMD. *J. Bone Miner. Res. Off. J. Am. Soc. Bone Miner. Res.* **2006**, *21*, 1464–1474. [[CrossRef](#)] [[PubMed](#)]
18. Xie, L.; Rubin, C.; Judex, S. Enhancement of the adolescent murine musculoskeletal system using low-level mechanical vibrations. *J. Appl. Physiol.* **2008**, *104*, 1056–1062. [[CrossRef](#)] [[PubMed](#)]
19. Hwang, S.J.; Lublinsky, S.; Seo, Y.K.; Kim, I.S.; Judex, S. Extremely small-magnitude accelerations enhance bone regeneration: A preliminary study. *Clin. Orthop. Relat. Res.* **2009**, *467*, 1083–1091. [[CrossRef](#)] [[PubMed](#)]
20. Pollak, A.N.; Powell, E.T.; Fang, R.; Cooper, E.O.; Ficke, J.R.; Flaherty, S.F. Use of negative pressure wound therapy during aeromedical evacuation of patients with combat-related blast injuries. *J. Surg. Orthop. Adv.* **2010**, *19*, 44–48. [[PubMed](#)]
21. Weinheimer-Haus, E.M.; Judex, S.; Ennis, W.J.; Koh, T.J. Low-intensity vibration improves angiogenesis and wound healing in diabetic mice. *PLoS ONE* **2014**, *9*, e91355. [[CrossRef](#)] [[PubMed](#)]
22. Novak, M.L.; Weinheimer-Haus, E.M.; Koh, T.J. Macrophage activation and skeletal muscle healing following traumatic injury. *J. Pathol.* **2014**, *232*, 344–355. [[CrossRef](#)] [[PubMed](#)]
23. Judex, S.; Lei, X.; Han, D.; Rubin, C. Low-magnitude mechanical signals that stimulate bone formation in the ovariectomized rat are dependent on the applied frequency but not on the strain magnitude. *J. Biomech.* **2007**, *40*, 1333–1339. [[CrossRef](#)] [[PubMed](#)]
24. Grounds, M.D. The need to more precisely define aspects of skeletal muscle regeneration. *Int. J. Biochem. Cell Biol.* **2014**, *56*, 56–65. [[CrossRef](#)] [[PubMed](#)]
25. Cross, J.D.; Ficke, J.R.; Hsu, J.R.; Masini, B.D.; Wenke, J.C. Battlefield orthopaedic injuries cause the majority of long-term disabilities. *J. Am. Acad. Orthop. Surg.* **2011**, *19*, S1–S7. [[CrossRef](#)] [[PubMed](#)]
26. Owens, B.D.; Kragh, J.F., Jr.; Macaitis, J.; Svoboda, S.J.; Wenke, J.C. Characterization of extremity wounds in Operation Iraqi Freedom and Operation Enduring Freedom. *J. Orthop. Trauma* **2007**, *21*, 254–257. [[CrossRef](#)] [[PubMed](#)]
27. Wu, Y.; Zhao, R.C.; Tredget, E.E. Concise review: Bone marrow-derived stem/progenitor cells in cutaneous repair and regeneration. *Stem Cells* **2010**, *28*, 905–915. [[PubMed](#)]
28. Chan, Y.S.; Li, Y.; Foster, W.; Horaguchi, T.; Somogyi, G.; Fu, F.H.; Huard, J. Antifibrotic effects of suramin in injured skeletal muscle after laceration. *J. Appl. Physiol.* **2003**, *95*, 771–780. [[CrossRef](#)] [[PubMed](#)]
29. Cheng, M.; Nguyen, M.H.; Fantuzzi, G.; Koh, T.J. Endogenous interferon-gamma is required for efficient skeletal muscle regeneration. *Am. J. Physiol. Cell Physiol.* **2008**, *294*, C1183–C1191. [[CrossRef](#)] [[PubMed](#)]
30. Zhu, J.; Li, Y.; Shen, W.; Qiao, C.; Ambrosio, F.; Lavasani, M.; Nozaki, M.; Branca, M.F.; Huard, J. Relationships between transforming growth factor-beta1, myostatin, and decorin: Implications for skeletal muscle fibrosis. *J. Biol. Chem.* **2007**, *282*, 25852–25863. [[CrossRef](#)] [[PubMed](#)]
31. Garg, K.; Corona, B.T.; Walters, T.J. Losartan administration reduces fibrosis but hinders functional recovery after volumetric muscle loss injury. *J. Appl. Physiol.* **2014**, *117*, 1120–1131. [[CrossRef](#)] [[PubMed](#)]
32. Ichioka, S.; Yokogawa, H.; Nakagami, G.; Sekiya, N.; Sanada, H. In vivo analysis of skin microcirculation and the role of nitric oxide during vibration. *Ostomy Wound Manag.* **2011**, *57*, 40.
33. Lohman, E.B., 3rd; Petrofsky, J.S.; Maloney-Hinds, C.; Betts-Schwab, H.; Thorpe, D. The effect of whole body vibration on lower extremity skin blood flow in normal subjects. *Med. Sci. Monit.* **2007**, *13*, CR71–CR76. [[PubMed](#)]
34. Maloney-Hinds, C.; Petrofsky, J.S.; Zimmerman, G.; Hessinger, D.A. The role of nitric oxide in skin blood flow increases due to vibration in healthy adults and adults with type 2 diabetes. *Diabetes Technol. Ther.* **2009**, *11*, 39–43. [[CrossRef](#)] [[PubMed](#)]
35. Adams, J.A.; Mangino, M.J.; Bassuk, J.; Kurlansky, P.; Sackner, M.A. Regional blood flow during per acceleration. *Crit. Care Med.* **2001**, *29*, 1983–1988. [[CrossRef](#)] [[PubMed](#)]
36. Adams, J.A.; Moore, J.J.E.; Moreno, M.R.; Coelho, J.; Bassuk, J.; Wu, D. Effects of Periodic Body Acceleration on the In Vivo Vasoactive Response to N-w-nitro-L-arginine and the In Vitro Nitric Oxide Production. *Ann. Biomed. Eng.* **2003**, *31*, 1337–1346. [[CrossRef](#)] [[PubMed](#)]
37. Arashi, M.; Sugama, J.; Sanada, H.; Konya, C.; Okuwa, M.; Nakagami, G.; Inoue, A.; Tabata, K. Vibration therapy accelerates healing of Stage I pressure ulcers in older adult patients. *Adv. Skin Wound Care* **2010**, *23*, 321–327. [[CrossRef](#)] [[PubMed](#)]



38. Sari, Y.; Sanada, H.; Minematsu, T.; Nakagami, G.; Nagase, T.; Huang, L.; Noguchi, H.; Mori, T.; Yoshimura, K.; Sugama, J. Vibration inhibits deterioration in rat deep-tissue injury through HIF1-MMP axis. *Wound Repair Regen.* **2015**, *23*, 386–393. [[CrossRef](#)] [[PubMed](#)]
39. Kiel, D.P.; Hannan, M.T.; Barton, B.A.; Bouxsein, M.L.; Lang, T.F.; Brown, K.M.; Shane, E.; Magaziner, J.; Zimmerman, S.; Rubin, C.T. Insights from the conduct of a device trial in older persons: Low magnitude mechanical stimulation for musculoskeletal health. *Clin. Trials* **2010**, *7*, 354–367. [[CrossRef](#)] [[PubMed](#)]
40. Rubin, C.; Recker, R.; Cullen, D.; Ryaby, J.; McCabe, J.; McLeod, K. Prevention of postmenopausal bone loss by a low-magnitude, high-frequency mechanical stimuli: A clinical trial assessing compliance, efficacy, and safety. *J. Bone Miner. Res. Off. J. Am. Soc. Bone Miner. Res.* **2004**, *19*, 343–351. [[CrossRef](#)] [[PubMed](#)]
41. Rubin, C.; Turner, A.S.; Bain, S.; Mallinckrodt, C.; McLeod, K. Anabolism. Low mechanical signals strengthen long bones. *Nature* **2001**, *412*, 603–604. [[CrossRef](#)] [[PubMed](#)]
42. Luu, Y.K.; Capilla, E.; Rosen, C.J.; Gilsanz, V.; Pessin, J.E.; Judex, S.; Rubin, C.T. Mechanical stimulation of mesenchymal stem cell proliferation and differentiation promotes osteogenesis while preventing dietary-induced obesity. *J. Bone Miner. Res. Off. J. Am. Soc. Bone Miner. Res.* **2009**, *24*, 50–61. [[CrossRef](#)] [[PubMed](#)]



© 2017 by the authors. Licensee MDPI, Basel, Switzerland. This article is an open access article distributed under the terms and conditions of the Creative Commons Attribution (CC BY) license (<http://creativecommons.org/licenses/by/4.0/>).